



**ADDIS ABABA UNIVERSITY**  
**SCHOOL OF GRADUATE STUDIES**  
**DEPARTMENT OF EARTH SCIENCES**

**HOLOCENE PALEOCLIMATE RECONSTRUCTION INFERRED FROM  
PROXY RECORDS IN SPELEOTHEMS FROM THE MECHARA KARST  
AREA AND LAKE ARCHIVES FROM TILO AND AWASSA LAKES,  
ETHIOPIA**

**A THESIS SUBMITTED TO THE SCHOOL OF GRADUATE STUDIES OF  
ADDIS ABABA UNIVERSITY IN PARTIAL FULFILLMENT OF THE  
REQUIREMENTS FOR THE DEGREE OF MASTER OF SCIENCE IN  
GEO-ENVIRONMENTAL SYSTEMS ANALYSIS**

***BY: AYNALEM ZENEBE***

***JULY 2009,***

***ADDIS ABABA, ETHIOPIA***

Addis Ababa University  
School of Graduate Studies  
Department of Earth sciences

**HOLOCENE PALEOCLIMATE RECONSTRUCTION INFERRED FROM  
PROXY RECORDS IN SPELEOTHEMS FROM THE MECHARA KARST  
AREA AND LAKE ARCHIVES FROM TILO AND AWASSA LAKES,  
ETHIOPIA**

**By: Aynalem Zenebe**  
**Department of Earth sciences**

**Approved by examining board:**

**Signature**

**1. Dr. Asfawossen Asrat**

**(Advisor)**

---

**2. Dr. Mohammed Umer**

**(Advisor)**

---

**3. Dr. Balemual Atnafu**

**(Internal Examiner)**

---

**4. Dr. Zewdu Eshetu**

**(External Examiner)**

---

## ***Acknowledgements***

*First, I would like to acknowledge my advisor Dr. Asfawossen Asrat for his all rounded help, deep consultation and follow up since the start of my work. I appreciate his great support in providing me all the stalagmite data, journals and references for this work. I would also like to thank him for his support during the field session to the Mechara caves. I would like to extend my gratitude to my second advisor, Dr. Mohammed Umer, for his keen advice and support through out my work. He has provided all the lake isotope data and other references for this work. I will always remember the kind help of my advisors and thank them heartily! I would like to extend my thanks to Solomon Kassa for his help during the statistical analysis.*

*I would also like to thank Addis Ababa University, Science Faculty, for the financial support for field work.*

*Last, but not least, I am also grateful to all my family, Emaye, Tsige, Zenebe, and my Hiwi, for you are with me all the time.*

## **Abstract**

*Holocene palaeoclimate records recovered from Bero\_1 stalagmite of Holocene age, and, modern stalagmite samples Asfa\_3, Ach\_1 and Merc\_1 and from lake Tilo and lake Awassa were compared in order to see the trends and nature of correlation and variability between the records. The major proxies used are the  $\delta^{18}\text{O}$  of Bero\_1 stalagmite together with the lamina width variation and the  $\delta^{18}\text{O}$  of authigenic calcite from the lake records, and lake level variations reconstructed from the Ziway-Shalla lakes. The  $\delta^{18}\text{O}$  proxy data was chosen because it varies with the variation in the precipitation amount and P/E ratios. The comparison made between  $\delta^{18}\text{O}$  values of stalagmites showed they are poorly correlated. The comparison of  $\delta^{18}\text{O}$  values between the Lake records and Bero\_1 stalagmite again showed poor correlation. But the over all trend of isotopic variation between the lake and stalagmite records in the Holocene was similar in such a way that it is similar with the general early-middle-late Holocene moisture variation previously recovered from Paleo-lake level variations of the Ziway-Shalla lakes. The stalagmite  $\delta^{18}\text{O}$  time series showed five major trends at a time scale of 100-120 years between 7800-7500, 7400-7300, 5400-5300, 4860-4800, and 4550-4470 yr BP and smaller variations at 10-20 years time scale within the major trends. Relatively enriched  $\delta^{18}\text{O}$  values in Bero\_1 stalagmite around 7650-7370 yr BP, 5300-5400, 4801-4860 and 4470-4530 yr BP and the recent late Holocene peak at the end of the growth phase correspond to the relatively lower precipitation periods in the Holocene. Similarly, the depleted  $\delta^{18}\text{O}$  values between 7590-7450, 5890-5860, 5290-5320 corresponds to relatively wetter periods. Thicker stalagmite lamina deposited during relatively wet seasons and thinner lamina records during relatively dry periods further support the  $\delta^{18}\text{O}$  trends with the precipitation amount variation. The  $\delta^{18}\text{O}$  of authigenic carbonates from lake Tilo and Awassa also showed similar relatively depleted  $\delta^{18}\text{O}$  values in the early Holocene wet period, and enriched values were recorded in dryer periods in response to the increased lake water evaporation effect. This study shows the comparison made between lake and stalagmite records follow similar trends through out the Holocene but with different magnitude of change; and the stalagmite records are further more important in providing a high resolution multi proxy records in order to understand the precipitation amount variability in the Holocene.*

## Table of contents

Chapter 1: Introduction .....	1
1.1 Theoretical background .....	1
1.1.1 Karst and the carbonate system.....	1
1.1.2 Cave carbonate deposits .....	3
1.1.3 Palaeoclimate significance of speleothems .....	4
1.2 Lake palaeoclimate records .....	5
1.3 Isotopes in palaeoclimate study .....	5
1.4 Objectives of the study .....	7
1.5 Expected outputs .....	8
Chapter 2: Literature review.....	9
2.1 Speleogenesis.....	9
2.2 Speleothem palaeoclimate records .....	9
2.3 Stable isotopes .....	11
2.3.1 Oxygen isotopes .....	13
2.3.2 Carbon isotopes.....	16
2.4 Lake records .....	17
2.5 Holocene Palaeoclimate of Ethiopia .....	19
Chapter 3: Site description and methodology.....	21
3.1 Location.....	21
3.2 The Mechara karst area and description of caves .....	21
3.2.1 The Achere-Ayange cave system.....	21

3.2.2 Rukiessa cave system .....	22
3.2.3 The Bero cave system.....	22
3.3 Geological Setting.....	25
3.4 Vegetation history.....	25
3.5 Climate .....	25
3.6 Lake sites .....	26
3.6.1 Lakes Tilo and lake Awasa .....	26
3.7 Methodology.....	26
Chapter 4: Results and Discussion .....	30
4.1 Results .....	30
4.1.1 Stalagmites.....	30
4.2 Stable Isotopes .....	31
4.2.1 Asfa-3 Stalagmite.....	31
4.2.2 Merc-1 stalagmite.....	32
4.2.3 Ach-1 stalagmite.....	33
4.2.4 Bero_1 stalagmite.....	34
4.2.5 Bero_1 growth phase_1 .....	35
4.2.6 Bero_1 Growth Phase_2.....	36
4.2.7 Bero_1 growth phase_3 .....	37
4.2.8 Bero_1 growth phase_4 .....	38
4.2.9 Bero_1 growth phase_5 .....	40
4.2.10 Bero_1growth phase_6 .....	41
4.3 Brro_1 Lamina width.....	42
4.4 Hiatuses.....	44

4.5 Equilibrium Condition .....	45
4.6 Lake Tilo Core .....	46
4.7 Lake Awassa core .....	49
4.8 Discussion .....	51
4.9 Comparison of stalagmite Records .....	53
4.10 Comparison of speleothem Vs lake isotope records .....	55
4.10.1 Comparison parameters:.....	55
4.10.2 Bero_1 stalagmite Vs Lake Tilo isotope record .....	57
4.10.3 Bero_1 growth phase_1 vs. Unit TL-1 .....	57
4.10.4 Bero_1 growth phase_2, 3, 4, 5 Vs Unit TL-2 .....	58
4.10.5 Bero_1 stalagmite Vs Lake Awassa isotope record.....	60
4.10.6 Comparison of Lake level variation with Speleothem isotope trends .....	61
Chapter 5: Conclusion and Recommendations .....	65
5.1 Conclusions.....	65
5.2 Recommendations .....	66

## List of Figures

Figure 1: The CO <sub>2</sub> -H <sub>2</sub> O-CaCO <sub>3</sub> system, modified after Fairchild et al., 2006 a .....	3
Figure 2: Location map of study sites .....	24
Figure 3: scanned image of Ach-1 Stalagmite.....	28
Figure 4: scanned image of Asfa-3 stalagmite .....	29
Figure 5: Scanned image of Merc_1 stalagmite. ....	29
Figure 6: Scanned image of Bero-1 stalagmite (left) and its schematic diagram (right).....	30
Figure 7: Asfa-3 stalagmite time series (a) and correlation of $\delta^{18}O$ Vs $\delta^{13}C$ (b) .....	31

Figure 8: Merc-1 stalagmite time series (a) and correlation of $\delta^{18}\text{O}$ Vs $\delta^{13}\text{C}$ (b).....	32
Figure 9: Ach-1 stalagmite time series (a) and correlation of $\delta^{18}\text{O}$ Vs $\delta^{13}\text{C}$ (b) .....	33
Figure 10: Bero_1 stalagmite $\delta^{13}\text{C}$ and $\delta^{18}\text{O}$ time series, green columns numbered H-1 to H-5 represent hiatuses .....	34
Figure 11: Bero_1 growth phase_1 time series (a) and correlation of $\delta^{18}\text{O}$ Vs $\delta^{13}\text{C}$ (b) .....	35
Figure 12: Bero_1 growth phase_2 time series (a) and correlation of $\delta^{18}\text{O}$ Vs $\delta^{13}\text{C}$ (b) .....	36
Figure 13: Bero_1 growth phase_3 time series (a) and correlation of $\delta^{18}\text{O}$ Vs $\delta^{13}\text{C}$ (b) .....	37
Figure 14: Bero_1 growth phase_4 time series (a) and correlation of $\delta^{18}\text{O}$ Vs $\delta^{13}\text{C}$ (b) .....	38
Figure 15: Bero_1 growth phase_5 time series (a) and correlation of $\delta^{18}\text{O}$ Vs $\delta^{13}\text{C}$ (b) .....	40
Figure 16: Bero_1 growth phase_6 time series (a) and correlation of $\delta^{18}\text{O}$ Vs $\delta^{13}\text{C}$ (b).....	41
Figure 17: Bero_1 stalagmites Lamina width against $\delta^{18}\text{O}$ , showing lamina width response oppositely with $\delta^{18}\text{O}$ ; Blue bars H-1 to H-5, represent hiatuses.....	43
Figure 18: Bero_1 stalagmites Lamina width Vs $\delta^{18}\text{O}$ correlation of Bero_1 growth phases 1-6.	43
Figure 19: Hendy tests for Asfa_3, Asfa_4, Merc_1 and Bero_1 stalagmites .....	46
Figure 20: Lake Tilo isotope record.....	48
Figure 21: Lake Awassa isotope record .....	50
Figure 22: Lamina width Vs $\delta^{18}\text{O}$ , with the 10 period moving average line of $\delta^{18}\text{O}$ (green), Lamina width (blue) and growth phases_1 to 6. ....	53
Figure 23: Asfa_3, Merc_1 and Bero_1 $\delta^{18}\text{O}$ and $\delta^{13}\text{C}$ comparison .....	54
Figure 24: Bero_1 Vs unit TL-1 comparison.....	58
Figure 25: Bero_1 Vs Lake Tilo Holocene isotope trends, arrows showing points of major isotope changes. ....	59
Figure 26: Lake Awassa isotope (red line) Vs Bero_1 isotope comparison .....	61
Figure 27: Lake Awassa, Lake Tilo and Bero_1 stalagmite Holocene isotope trends.....	64

## **List of tables**

Table 1: summary of caves, modified after Asrat et al., 2008

## **List of acronyms**

ITCZ: Inter Tropical Convergence Zone

IAEA: International Atomic Energy Agency

PDB: Pee Dee Belemnite

VSMOW: Vienna Standard Mean Oceanic Water

NERC: National Environmental Research Center

Cal Kyr: Calculated Kilo Year

TDIC: Total Dissolved Inorganic Carbon

MER: Main Ethiopian Rift

Yr BP: Years before present

M a.s.l: Meters above sea level

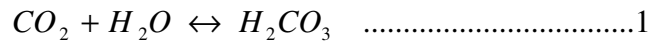
# Chapter 1: Introduction

## 1.1 Theoretical background

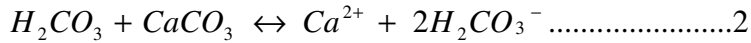
### 1.1.1 Karst and the carbonate system

Karst can be defined as a terrain with distinctive hydrology and landform that arises from a combination of high rock solubility and well developed secondary porosity (fracture systems). Karst areas are characterized by sinking streams, caves, enclosed depressions, fluted rock outcrops and large springs (Ford & Williams, 2007). Karsts are best developed in carbonate rock terrain with extensive exposures of limestone (composed of calcite and aragonite) and dolostone (dolomite). In Ethiopia, extensive limestone beds with great potential for caving are exposed in three major sedimentary basins of the country; the Mekelle outlier in the north (Tigray), the Blue Nile basin and the Ogaden Basin (including the west Hararge Mechara karst region) (Asrat *et al.*, 2008).

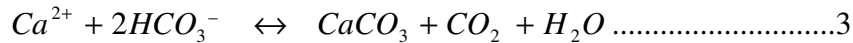
It will be of great relevance to understand the karst system in detail in order to have a clear view of the processes that operate in this environment. Karsts are best understood from the system perspective and they can be viewed as an open system composed of two closely integrated hydrological and geochemical subsystems operating up on the karstic rock. Karst features observed above and below the ground are the products of the interplay of the processes in these linked subsystems. The system as a whole is divided into two zones based on the different geochemical processes operating. The upper zone of dissolution includes the soil zone together with the highly fractured surface rock called the epikarst or the subcutaneous zone. The epikarst acts as a perched aquifer which feeds both major conduits and low transmissivity fissures which in turn feed the zone of drip water in the cave. The soil zone plays a key role in the carbonate system as it is the major source of CO<sub>2</sub> which reacts with percolating water to form carbonic acid which later dissolves the carbonate bedrock.



*percolation through the soil zone and the epikarst*



The epikarst zone is the zone of dissolution where the soil and upper epikarst is dominated by carbonate dissolution in contact with waters of higher dissolved CO<sub>2</sub> (P<sub>CO2</sub>) derived from plant root respiration and microbial decay of organic matter (litter fall) in the soil zone. Meteoric water, already containing small proportion of atmospheric CO<sub>2</sub>, mixes with soil carbon dioxide to form weak carbonic acid (H<sub>2</sub>CO<sub>3</sub>) which acts to dissolve away the limestone bedrock. Beneath the epikarst lies the zone of carbonate precipitation. This region is the zone of carbonate supersaturation and speleothem precipitation derived by CO<sub>2</sub> degassing from percolating water in to the cave atmosphere which is relatively with lower (P<sub>CO2</sub>) (Fairchild *et al.*, 2006 a).



The process of CO<sub>2</sub> degassing in to the cave air leads to supersaturation of the solution with respect to calcite and as a result calcite is precipitated out of solution. The process of carbonate precipitation in the cave is a very important stage where the important palaeoenvironmental and palaeoclimate signals are transferred to be held in the calcite precipitate. However, the climate signals could be modified by the karst aquifer and cave environment in mixing, storing and delivering water (percolation route) to the site of speleothem formation.

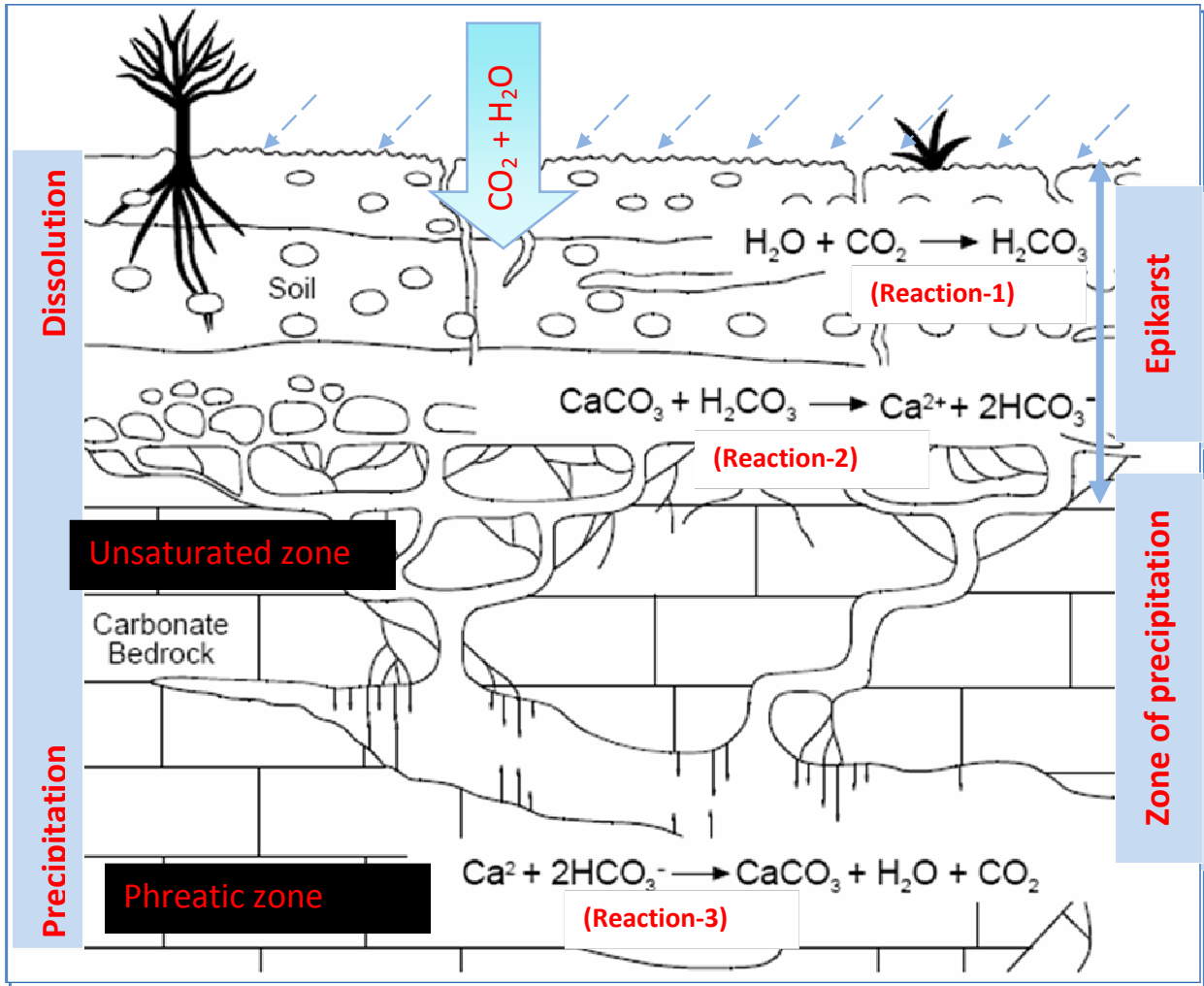


Figure 1: The CO<sub>2</sub>-H<sub>2</sub>O-CaCO<sub>3</sub> system, modified after Fairchild et al., 2006 a

### 1.1.2 Cave carbonate deposits

In the process of CO<sub>2</sub> degassing in the cave, three principal types of carbonate precipitates are formed collectively known as speleothems. This includes flow stones, laminated deposits on the wall and floor of the cave that form due to the sheet of flowing water derived from fissures and conduits. Though their lateral extension allows repeated sampling for palaeoclimate studies, flow

stones are less frequently used because they are difficult to date due to their high impurity content. In addition flowstones show complex internal stratigraphy and non uniform calcite growth rate.

The second group of speleothems is stalactites, which grow associated with seepage zones connected with the epikarst above the cave. Hollow cylindrical Soda straw stalactites are very delicate and record the youngest few decades of the cave record. Stalactites growing on the ceiling of the cave are naturally fallen on the cave floor, and hence preferred by researchers for conservation reasons (Fairchild *et al.*, 2006a).

Stalagmites grow upwards from the cave floor as the seepage water precipitates down from the stalactite surface. Stalagmites are most favored by researchers because their simple geometry which depends on the seepage flow rate, degree of supersaturation and drop fall height. They are studied in polished sections; these stalagmites reveal a stratigraphy which reflects the growth of the stalagmite as a function time.

### **1.1.3 Palaeoclimate significance of speleothems**

In recent years, speleothems have received great deal of attention in palaeoclimate studies because they can grow for long geologic time,  $10^3$ - $10^5$  years, providing a continuous and multi proxy continental climate records. In addition, speleothem climate records show little secondary alteration after they are recorded in the cave calcite. Such records in speleothems are accurately dated to a precision of  $\pm 1\%$  from samples of less than 1g of calcite, due to the recent development of thermal ionization mass spectrometric (TIMS) U-series dating. (Ayalon A. *et al.*, 1999) The various palaeoclimate proxy records recovered from speleothems include stable isotopes (both  $\delta^{18}\text{O}$  and  $\delta^{13}\text{C}$ ), trace element records, laminae fluorescence index, stalagmite morphology, laminae thickness and growth rate variation (Fairchild *et al.*, 2006a ; Asrat *et al.*, 2007) some of which will be discussed in detail in the coming sections.

Cave calcite deposits contain climate signals because climate is the major controlling factor in speleogenesis for the following reasons. Firstly, climate controls the chemistry and/or quantity of water in the water cycle which plays major role in speleothem formation. Together with altitude and topography, it also influences chemistry of the carbonate system and the soil properties,  $\text{CO}_2$

transport and aquifer recharge. All these factors will be reflected in the chemical composition and rate of growth of the stalagmites and interpreted as a climate proxy.

## **1.2 Lake palaeoclimate records**

Past lake level variations are perhaps the most important sources of information regarding Late Pleistocene-Holocene climate change in east Africa and Ethiopia. A good example is the Holocene record of climate variability from the Ziway-Shala Lakes in the Main Ethiopian Rift (MER) and Lake Abh'e in the Afar (Lamb *et al.*, 2000; Mohammed *et al.*, 2004). And, in recent years, there are centennial to decadal resolution climate signals recovered from Lake-core records in other small crater Lakes in the rift and few highland Lakes (from Lakes Tilo, Hora and Haik) (Lamb *et al.*, 2004; Lamb *et al.*, 2006). There are several factors that control the sensitivity of Lakes to climate variability. Lakes that are highly sensitive to changes in climate include Lakes with no surface outlet or closed basin Lakes. Hence, crater Lakes and Lakes in fault bounded basin are especially sensitive to climate change because they are often considered closed and their water balance respond almost fully to changes induced by climate. In addition, they have steep sides so that Lake level change can easily be observable. In this case, the Ethiopian Rift Valley has a number of such Lakes and thus it is an ideal place for climate change reconstruction studies. Yet, serious care must be taken to sort out non climate effects on Lake sediment records like volcanic activity and tectonics (Lamb *et al.*, 2002). The commonly used Lake climate proxy data, in addition to past Lake level includes stable isotope records (both  $\delta^{18}\text{O}$  and  $\delta^{13}\text{C}$ ) recovered from core samples of Lake sediments and autogenic calcite deposits, pollen data (species and abundance), and Lake diatom data (species, abundance and isotope composition of their shale). The detail of the Lake proxy data that will be used in this study will be discussed later in detail.

## **1.3 Isotopes in palaeoclimate study**

Systematic study of stable isotopes in speleothems commenced more than three decades ago, and has developed more in recent years with the development of new dating techniques (McDermott *et al.*, 2004). Among the most commonly used stable isotopes in climate and environmental changes are O, H, C, N and S, because these elements are found abundant in our environment. Stable isotope composition comprises the major type of geochemical investigation of

speleothems assuming that cave interiors exactly approximate the surface climatic condition (Fairchild *et al.*, 2006a). Isotopes of O and C are powerful tracers of climate change. Particularly, O isotopes are widely used in palaeoclimate studies because they are more readily fractionated than C isotopes do. Never the less, it is very difficult to measure actual concentration of isotopes in a sample. Hence, the ratios of the most abundant stable isotope of a particular element are measured relative to a standard containing the element in which the isotopic ratio is known. The ratios are expressed in delta value ( $\delta$ ) according to the equation

$$\delta = \frac{R_{sample} - R_{standard}}{R_{standard}}$$

Where,  $R_{sample}$  is the  $\delta^{18}\text{O}/\delta^{16}\text{O}$  or  $\delta^2\text{H}/\delta^1\text{H}$  ratio of the sample and  $R_{standard}$  for the corresponding ratio in the standard VSMOW (Freidman and O'Neil., 1977; Darling and Talbot., 2003). For example, for Oxygen isotopes,  $R_s$  is the ratio of  $^{18}\text{O}$  to  $^{16}\text{O}$ . Because of the small difference in isotopic ratio, the delta values are commonly multiplied by 1000 so that the resulting numbers are  $>1$  or  $< -1$  depending on the sign. Using this multiplication, the equation will be

$$\delta = \left( \frac{R_s}{R_r} - 1 \right) \times 1000 \text{‰}$$

The symbol ‰ meaning parts per thousand (permil) which the standard for  $^{18}\text{O}$  and  $^2\text{H}$  is known as VSMOW, stands for Vienna Mean Oceanic Water. This standard is maintained by the International Atomic Energy Agency (IAEA). The standard for Carbon was originally established using a fossil belemnite from the cretaceous Pee Dee limestone formation and abbreviated as PDB. This standard was inert calibrated by the IAEA and become VPDB. Similarly,  $^{18}\text{O}/^{16}\text{O}$ ,  $^2\text{H}/^1\text{H}$ , and  $^{13}\text{C}/^{12}\text{C}$  ratios from Lake waters, autogenic calcite, organic material and diatom silica are measured as relative differences and the ratios are expressed in terms of the delta ( $\delta$ ) notation (Anson Mackay., 1977). Both the VSMOW and the PDB standards can be used to report variation in oxygen isotope ratio  $\delta^{18}\text{O}$  value of calcite on the PDB and SMOW standard is related by the formulas;

$$\delta_{SMOW} = 1.03086\delta_{PDB} + 30.86 \quad \text{And} \quad \delta_{PDB} = 0.97006\delta_{SMOW} - 29.94$$

## 1.4 Objectives of the study

The general objective of this work is to compare palaeoclimate data (Holocene pattern of precipitation variation and dryness) obtained from high resolution, annually laminated stalagmite records from southeastern Ethiopia and Lake records from Lake Tilo and Lake Awassa in south Ethiopia. The comparison will be used to see the nature of Holocene climate variability recorded in stalagmite and lake sediments in the Holocene and, to test the trend of climate variability between the two proxies. The data comparison will be conducted in order to test the nature and trend of correlation within and between the different proxies ( $\delta^{18}\text{O}$  isotopes, and laminae thickness in speleothems) and  $\delta^{18}\text{O}$  isotopes, lake level variations, etc in lake records) in order to do statistical analysis which will be used to complement the low resolution Lake records and hiatus in the stalagmite records throughout the Holocene period. The correlation made between proxy records in the two archives will also help to point out the exact timing and duration of major climate change events (dry/wet episodes) identified in Lake records using precisely dated high resolution stalagmite records. This study will help to see the nature of Holocene climate variation in Ethiopia using secondary data from various published and unpublished previous research works. The result will provide a generalized overview of the Holocene climate trend in the region based on high resolution various multi-proxy data sources. The specific objectives of this study include:

1. To test the nature and trend of correlation among the different proxy records found in the stalagmite and lake sediments.
2. To examine the variability of the isotope ratio using the time series of  $\delta^{18}\text{O}$  from the Lake cores and the stalagmites over the overlapping period over the Holocene
3. To do a statistical analysis based on the correlation between the stalagmite and lake  $\delta^{18}\text{O}$  data and compare with the trend of low resolution Lake isotope records using the annual resolution of stalagmite records.
4. To determine the frequency and timing of the dry and wet periods in the Holocene as identified from the proxy variation.

## **1.5 Expected outputs**

The following outputs are expected by the end of this research work.

- ❖ The nature of major climate shift in the Holocene is understood together with the precise timing and duration of the major climate shift.
- ❖ The magnitude of Holocene climate variability between the two archives will be compared.
- ❖ The proxy data obtained from stalagmite and lake records will be statistically tested to determine the nature of correlation this will contribute to the understanding of Holocene climate at a high temporal resolution.
- ❖ The result will help as background information to the understanding of past drought events in Ethiopia.

## **1.6 Hypothesis**

Speleothems are excellent sources of paleoclimate data. The oxygen and carbon isotope data together with the lamina width variation preserved in the speleothem calcite provide the change in the precipitation amount and the vegetation change in an area respectively. Similarly, lake records including oxygen and carbon isotopes and Paleo-lake level changes provide important information about the variation in precipitation and evaporation, and based on this, periods of dry/wet climate conditions can be reconstructed. Previous paleoclimate research work conducted in Ethiopia focused on lake archives and recently on speleothem archives. Yet the nature of correlation and the trend of climate variation between the two paleoclimate archives is not compared and studied. It is important to test the nature and trend of isotope variation variations between the two archives with different time resolution in order to reconstruct the Holocene climate variation.

## Chapter 2: Literature review

### 2.1 Speleogenesis

Speleothems, stalactites and stalagmites formed inside caves, consist of calcium carbonate precipitated from cave waters that are supersaturated with respect of calcite (fig.1). Supersaturation in most cases is achieved by degassing of carbon dioxide ( $\text{CO}_2$ ) from drip waters which enter the cave through fractures that connect with the epikarst and the soil zone above the cave.  $\text{CO}_2$  degassing occurs because the water was previously equilibrated with  $\text{CO}_2$  at elevated partial pressure in the soil percolation zone and degasses up on emergence into the lower  $P_{\text{CO}_2}$  of the cave atmosphere which is almost always somewhat ventilated (relative to the soil atmosphere) (Lauritzen and Lundberg., 1999; Kaufmann and Dreybrodt., 2004). As the seepage water releases  $\text{CO}_2$  in the cave atmosphere, the percolating water will be supersaturated towards calcite and  $\text{CaCO}_3$  will be precipitated forming speleothems. The  $\delta^{18}\text{O}$  and  $\delta^{13}\text{C}$  values of speleothem calcite reflect primary environmental conditions as long as equilibrium fractionation of the isotopes occurred between the drip water and calcite minerals. Other kinetic and/or evaporative processes may mask these primary environmental variables and usually Hendy test and replication tests are conducted on any stalagmite sample prior to palaeoclimate study in order to check for kinetic fractionation effects (Doralle *et al.*, 2001).

### 2.2 Speleothem palaeoclimate records

In order to understand our past climate and predict the future accurately, there is a need for improved palaeoclimate records with both high spatial and temporal resolution (Fairchild *et al.*, 2005). Speleothems, in this regard, bear valuable palaeoclimate information in terms of variation in their chemical and stable isotope composition through time. A number of biogeochemical proxies in speleothems can be used to extract palaeoclimatic information (Lauritzen and Lundberg., 1999; Bar-Mathews *et al.*, 2003; Fairchild *et al.*, 2006a; Asrat *et al.*, 2007). Among them, the most commonly used is oxygen isotope variation ( $\delta^{18}\text{O}$ ) which is a function of (1) depositional temperature that affects oxygen fractionation between water and calcite and (2) the oxygen isotope composition of cave drip water, which is closely related to the isotopic composition of the local precipitation. The second parameter is a function of long term cumulative change in a number of competitive factors, including, the  $\delta^{18}\text{O}$  of moisture content in

the seawater, temperature gradient between the sites of moisture source and precipitation, vapor condition temperature in clouds, and the amount of precipitation affecting isotope exchange in rain drops (Emiliani *et al.*, 1966; Lauritzen and Lundberg., 1999; Xia *et al.*, 1999; Fairchild *et al.*, 2001; Genty *et al.*, 2002).

The second most important climate proxy in speleothems is the carbon isotope composition, which is usually related to the relative abundance of plants using C<sub>3</sub> photosynthetic pathway versus C<sub>4</sub> plants (Fairchild *et al.*, 2006a; Mickler *et al.*, 2006).

Speleothem growth rate is another important palaeoclimatic indicator which is a function of drip water Ca content, water supply and the soil CO<sub>2</sub> concentration, all of which are climatically controlled. Water supply (drip rate) is directly related with effective precipitation (rainfall-evaporation). Soil CO<sub>2</sub> concentration is a function of plant productivity, which is related to both temperature effective precipitation and atmospheric CO<sub>2</sub>. Ca concentration in drip water is controlled by temperature and groundwater flow path (Xia *et al.*, 1999; Dorale *et al.*, 2001; Frisa *et al.*, 2003)

Additional proxies that speleothems provide include laminae width, fluorescence wavelength, trace element ratios and pollen data. (Baker *et al.*, 1998; Roberts *et al.*, 1998; Baker and Genty *et al.*, 1999; Baker *et al.*, 2002; Bertaux *et al.*, 2002; Proctor *et al.*, 2002; Kaufmann and Dreybrodt., 2004; Asrat *et al.*, 2007)

Fluorescence occurs when molecules with high energy levels release energy in the form of light after excitation by UV light (McGarry and Baker *et al.*, 2000). Fluorescence is generated by organic acids (humic /fluvic) from decomposed plants in the overlying soil. Climate is among the many factors that control organic matter content of a soil mummifications. Soil moisture content and temperature control organic acid content of the soil and the groundwater feeding the cave speleothem deposits (Baker and Genty., 1999).

The growth rate of stalagmites contains a potential palaeoclimate signal as the chemical kinetics of stalagmite growth is dependent on several variables which can be determined by the climate and vegetation changes. Stalagmite growth rate is controlled by CO<sub>2</sub> variation (as a proxy of soil activity), drip water calcium content, and drip rate (as a proxy of precipitation). But in most cases, growth rate is incorporated with other records contained within speleothem calcite in order to obtain multi-proxy record of palaeoclimate change (Baker *et al.*, 1998; Asrat *et al.*, 2007).

Annual growth laminae in stalagmites are recognized as high resolution archives of climate proxies. The formation of annual laminae reflects seasonal changes in drip water chemistry and/or seasonal changes in cave air carbon dioxide concentration, which alter the saturation state and, therefore, the fabric of carbonate that precipitated. It has been observed that annual laminae development depends on seasonal flushing of soil-derived elements, particles and organic matter. Hence, temporal changes in the growth rate of stalagmites is controlled by aspects of surface precipitation (annual effective precipitation) and annual growth laminae are thus used to derive long rain records. According to Asrat *et al.*, 2007, the occurrence of continuous lamina sequence in stalagmites is most frequently indicative of an annual climate forcing. Accordingly, he explained this idea using annually laminated Holocene age stalagmite from the Mechara karst area in south-east Ethiopia (a region having a strongly seasonal climate with a summer period of water excess) annually laminated and forced by seasonal variation of water excess (Asrat *et al.*, 2007)

There are a number of advantages that speleothems have over other palaeoclimate archives like Lake sediments and peat cores (McDermott, 2004). In this regard, speleothems have preservational and dating advantages. Because of the closed crystalline nature of the speleothem calcite, the climate records are usually not susceptible to secondary alterations like contamination or degradation. In addition, because of their situation underground, speleothem deposits are protected from external erosion and may remain undamaged for long period of geologic time (Lauritzen and Lundberg., 1999; Williams *et al.*, 2004; Fairchild *et al.*, 2006 a). Most speleothems can be accurately dated back to 400-600 Ka Bp by U-series dating methods allowing climate proxies to be placed in to accurate chronological framework in which case a precise chronology can be tied to stalagmite stratigraphy (Xia *et al.*, 2001; Genty *et al.*, 2002; McDermott., 2004; Williams *et al.*, 2004., Mckler *et al.*, 2006.).

## 2.3 Stable isotopes

Carbon and Oxygen isotopes in speleothems have been studied for more than three decades commonly with the central goal of reconstructing past environmental and/or climatic conditions (Doralle *et al.*, 2001; McDeromtt *et al.*, 2004). Because of their link to the hydrologic cycle, the soil system and the biosphere; speleothems are capable of preserving meteoric water oxygen isotope signature and the soil CO<sub>2</sub> variations respectively. Isotopic composition of speleothem calcite is a function of cave external and cave internal primary environmental conditions including conditions above the cave like the drip water composition modified by geographical location, weather conditions, surface biosphere and soil conditions as well as the thermal and evaporative conditions within the cave.

According to Hendy, 1971 (cited in Dorale *et al.*, 2001; Mickler *et al.*, 2006) although it is clear that  $\delta^{18}\text{O}$  is affected by temperature and the isotopic composition of meteoric precipitation, and that of  $\delta^{13}\text{C}$  is affected by isotopic composition of soil organic matter, it is also possible that other non climate processes may mask these primary environmental variables during calcite crystallization. In this regard, the reliability with which the  $\delta^{18}\text{O}$  and  $\delta^{13}\text{C}$  values of the speleothem calcite reflect only environmental variables is a complex issue (Dorale *et al.*, 2001, McDeromtt *et al.*, 2004; Fairchild *et al.*, 2006a). Hence, even though speleothem isotopic records provide a huge set of palaeoclimatic and palaeoenvironmental information, it is critical to understand the factors that control isotope fractionation during speleothem calcite precipitation (Hellstorm *et al.*, 1998, Mickler *et al.*, 2006)

There are two types of isotopic fractionation in speleothem deposition, in high humidity cave interiors with no evaporation or in conditions of slow CO<sub>2</sub> degassing rates, the isotopes in the calcite crystals are deposited in thermodynamic equilibrium with drip water, which means that the distribution of light and heavy isotopes between the aqueous and solid phase is only a function of temperature (Lauritzen and Lundberg., 1999; Dorale *et al.*, 2001; Williams *et al.*, 2004). In evaporative conditions or fast rate of crystallization due to high Ca supersaturation, the isotopic fractionation between the two phases is controlled by kinetic effects rather than by temperature. Both situations reflect climatic conditions and can be used as climate proxies, but the equilibrium situation is much simpler and easier to interpret because under such conditions, temporal variations in  $\delta^{18}\text{O}$  and  $\delta^{13}\text{C}$  values most likely reflect changes in the primary

environmental variables of interest, not in varying degrees of non-equilibrium effects (Thompson *et al.*, 1974; Lauritzen and Lundberg., 1999; Doralle *et al.*, 2001). A series of sub-samples from the same growth layer be analyzed from the center of the stalagmite progressively outward and down the sides if deposition takes place under equilibrium conditions,  $\delta^{13}\text{C}$  values should become progressively enriched from the center outward while  $\delta^{18}\text{O}$  values should remain essentially constant. This argument is valid because the reservoir of carbon atoms (mostly as bicarbonate) is limited relative to the reservoir of oxygen atoms (the water molecules themselves) (Bar-Mathews *et al.*, 1996; Mickler *et al.*, 2006.)

According to Hendi, 1971 (cited by Dorale *et al.*, 2001; Mickler *et al.*, 2006) the following are tests conducted to check whether the calcite was precipitated under thermodynamic equilibrium or not.

1.  $\delta^{18}\text{O}$  and  $\delta^{13}\text{C}$  values of samples along a single growth layer of a stalagmite should lack progressive increase away from the growth axis. Progressive increase in the  $\delta^{18}\text{O}$  value outwards from the center of the stalagmite may indicate evaporative enrichment on the stalagmite surface.
2.  $\delta^{18}\text{O}$  and  $\delta^{13}\text{C}$  values of samples taken along a single growth layer should not be positively correlated. Due to reservoir effects (limited amount of bicarbonate),  $\delta^{13}\text{C}$  will change progressively from the apex and down the sides of the stalagmite while  $\delta^{18}\text{O}$  will be invariant due to the relatively large amount of water available. (Lauritzen and undberg., 1999)
3. Samples taken along the growth axis should lack positive correlation in  $\delta^{18}\text{O}$  and  $\delta^{13}\text{C}$  values. In this case, however, both  $\delta^{18}\text{O}$  and  $\delta^{13}\text{C}$  values of calcite along growth axis could be positively correlated with environmental change.

Still the Hendy test is difficult to conduct practically because of the difficulties with physical sampling along the same growth layer as each layer get thinner outwards to the sides of the stalagmite. In addition to this, isotopic disequilibrium associated with rapid  $\text{CO}_2$  degassing and calcite precipitation would cause speleothems to fail these three tests. Hence, Dorale *et al.*, 2001 suggests that the replication test is more robust test to identify non equilibrium processes than the traditional Hendy test, as this test essentially rules out all of the non-equilibrium factors.

### 2.3.1 Oxygen isotopes

$\delta^{18}\text{O}$  variations in speleothem calcite can be indicative of both changes in temperature and changes in the isotopic composition of cave water, which is climatically controlled and directly related to that of the rain water composition (Bar-Matthews and Ayalon *et al.*, 1997; Mickler *et al.*, 2004). Oxygen isotopes in speleothem calcite have been used to determine temperature at the time of deposition, because the  $^{18}\text{O}/^{16}\text{O}$  in calcite during its precipitation is temperature dependent (Williams *et al.*, 1999, 2004). The temperature within the interior of the cave varies very little over the year and is very close to the mean annual air temperature (Williams *et al.*, 2004; Cai *et al.*, 2006) so, if the external mean annual air temperature changes over time, the cave temperature will adjust accordingly, and this will result in oxygen isotope ratio changes of the calcite being precipitated. Thus the oxygen isotope ratios of a stalagmite reflect temperature changes during its growth, if this occurred in isotopic equilibrium (Hellstorm *et al.*, 1998; Lieng *et al.*, 2001; Williams *et al.*, 2004).

In addition, speleothem  $\delta^{18}\text{O}$  values are used to reconstruct oxygen isotopic composition of cave drip water that is closely related to the mean local precipitation. This parameter is a function of a number of competing factors which interpretation of variations of  $\delta^{18}\text{O}$  in speleothem calcite requires the knowledge and quantitative estimation of processes that may affect the isotopic composition of water during the course of the hydrologic cycle and during calcite deposition (starting from evaporation from the sea surface, condensation precipitation at the cave site and calcite deposition out of the drip water) (Araguas *et al.*, 2000; Doralle *et al.*, 2001; Linge *et al.*, 2001; Williams *et al.*, 2004; Genty *et al.*, 2006;)

According to Lauritzen and Lundberg., 1999; Williams *et al.*, 1999 and Doralle *et al.*, 2001 the processes are categorized in to various “effects” as

1. The cave temperature effect which represents the thermodynamic fractionation between the drip water and the calcite during deposition. Friedman and O’Niel, 1977, cited by Doralle *et al.*, 2001, experimentally determined the temperature dependence of the fractionation as  $\sim -0.24\text{‰}$  per  $^{\circ}\text{C}$  meaning there will be greater fractionation at cold temperature relative to warm temperatures.

2. The rain water composition effect relates to the fate of the air mass on its route from the site of evaporation to the site of rainfall. It is a function of the storm tracks, called the rainout effect and of the temperature of the site of precipitation.
3. The ice-volume effect represents the change in isotopic composition of the ocean source during glacial/interglacial transitions when the seawater becomes more enriched as ice volume increases. This effect is more dominant during periods of large scale climate change like periods of glacial/interglacial fluctuation.
4. The ocean temperature effect reflects the temperature dependent fractionation between the liquid and the vapor phase at the source of atmospheric moisture, the Ocean.
5. The amount effect, where the  $\delta^{18}\text{O}$  value of the precipitation progressively diminish with increasing rainfall amount and/or intensity. This effect is pronounced in tropical monsoonal climate regions.
6. The extent of surface evaporation in the vadose zone (Lauritzen and Lundberg., 1999; Araguas *et al.*, 2000; Xia *et al.*, 2001; Williams *et al.*, 2004).

Yet the relative importance of these effects depends on the geographic location of the cave site and the temporal scale of climate change. In the first case for example, the cave temperature effect may either emphasize or oppose the rainwater composition effect. Rainwater composition effect is linked to temperature. The correlation between mean annual precipitation  $\delta^{18}\text{O}$  values and mean annual precipitation is strongest for high latitude regions where higher mean annual temperature correlates to higher mean annual precipitation  $\delta^{18}\text{O}$  values (Doralle *et al.*, 2001). In tropical and monsoonal climate areas, the amount effect is the most dominant process that affects the  $\delta^{18}\text{O}$  value of precipitation such that an increase in the amount of precipitation will result in precipitation with lower  $\delta^{18}\text{O}$  values (Bar-Mathews *et al.*, 1999; Doralle *et al.*, 2001; Burns *et al.*, 2003; Fleitmann *et al.*, 2003; Mickler *et al.*, 2006; Baker *et al.*, 2007). Similarly,  $\delta^{18}\text{O}$  values of precipitation in the Mechara Karst area in south east Ethiopia with strong seasonal monsoon

variability controlled by movement of the ITCZ, is influenced by the amount effect (Asrat *et al.*, 2007, Baker *et al.*, 2007)

### 2.3.2 Carbon isotopes

Carbon isotopic variation in speleothems reflects a variety of potential processes from which a primary environmental signal can be extracted. Each one of these specific process may dominate the other in specific situations (Doralle *et al.*, 2001; Fairchild *et al.*, 2006).

The primary source of carbon in the cave seepage water is the soil carbon dioxide, which is controlled by atmospheric CO<sub>2</sub>, plant respiration, and organic matter degradation; together with the bedrock carbonate (CaCO<sub>3</sub>) which is dissolved during seepage (Doralle *et al.*, 2001; Genty *et al.*, 2006; Johnson *et al.*, 2006). Biological activity in the soil horizon above the cave produces high level of CO<sub>2</sub> that will acidify seepage water which in turn dissolves carbonate bedrock enroute to the underlying caves. Variation in the  $\delta^{13}\text{C}$  values of calcite Speleothems mainly reflect changes of the vegetation type in the vicinity of a cave and vegetation at the regional scale is strongly correlated to climate (Bar-Matthews *et al.*, 2003; Baker *et al.*, 2007). These primarily reflect differences in the isotopic composition of C<sub>4</sub>- C<sub>3</sub> photosynthetic carbon fixation pathways, in that C<sub>3</sub> plants have  $\delta^{13}\text{C}$  values -23‰ to -33‰ and C<sub>4</sub> plants with  $\delta^{13}\text{C}$  value -9‰ to -16‰. Additional factors influencing the carbon isotopic composition of plants include temporal isotopic variations of atmospheric CO<sub>2</sub> due to increased fossil fuel C concentrations, plants stress due to water deficiency, and temperature (Bar-mathews *et al.*, 2003., Mickler *et al.*, 2006 ). Vegetation is a major factor because soil CO<sub>2</sub> is generated largely by the microbial oxidation of soil organic matter. C<sub>3</sub> and C<sub>4</sub> photosynthetic pathways produce large differences in  $\delta^{13}\text{C}$  values. C<sub>3</sub> plants have average  $\delta^{13}\text{C}$  values average of -26 ‰, whereas C<sub>4</sub> plants average ca. -13 ‰ (Doralle *et al.*, 2001; McDermott *et al.*, 2004; Fairchild *et al.*, 2006). At the same time, the isotopic composition difference between C<sub>3</sub> and C<sub>4</sub> plants is 15‰ which is sufficient to estimate the relative contribution of C<sub>3</sub> and C<sub>4</sub> plants C to the soil system.

Enrichment in the <sup>13</sup>C of the speleothems' calcite usually reflects an increase in the contribution of C<sub>4</sub> plants to the soil CO<sub>2</sub>. Under conditions of water deficiency, high environmental temperature, low atmospheric CO<sub>2</sub> concentration, or some combination of these, C<sub>4</sub> plants are more photosynthetically efficient than C<sub>3</sub> plants (Linge *et al.*, 2001; McDermott *et al.*, 2004;

Mickler et al., 2006). However, there is also a tendency for C<sub>3</sub> plants with high water use efficiency to be enriched in <sup>13</sup>C. Therefore, in arid environments, C<sub>3</sub> plants tend to have more positive δ<sup>13</sup>C values compared with those under less water-stressed conditions (Bar-Mathews et al., 2003). C<sub>4</sub> plants are entirely tropical grasses, while C<sub>3</sub> plants include all woody plants and high elevation grasses.

## 2.4 Lake records

Lake records have long been used in palaeoclimate and palaeoenvironmental studies in Ethiopia. Previous palaeoclimatic research in Ethiopia has been based on ancient shorelines and sediments of large rift valley Lakes (Mohammed, U., 1994; Mohammed and Bonnefille, 1998; Lamb *et al.*, 2000). Various studies conducted in the Holocene palaeoclimate variability revealed the cyclicity of dry/wet changes, and accordingly, higher Lake level stand was recorded at Early-mid Holocene in the Ziway and Shalla Lakes. These two Lakes, in the MER, together with Lake Abh'e in Afar, witnessed rise in level around 10.7-9.5 cal. Kyr due to the wetness as a result of orbitally induced increase in monsoon strength (Mohammed and Bonnefille, 1998; Mohammed *et al.*, 2004 and reference there in) However, this warm and wet condition was interrupted by short-lived dry conditions characterized by significant Lake level drops around 8.7-8.1, 6.7 and 5.5-4.5 kyr. This was similar for most of the Eastern African Lake level records (Lamb *et al.*, 2000; Mohammed *et al.*, 2004). Again, there was a return of wetter condition during the Late-Holocene; e.g., a rise of 70m was dated between 3.8-1.6 cal. Kyr at Lake Abh'e (Mohammed *et al.*, 2004) and Lake Shala rose by 42m above the present level around 1.9-1.4 cal Kyr.

Recently, the application of isotopes in palaeoclimate studies of crater Lakes is becoming more prevalent. The Main Ethiopian Rift valley is especially attractive site for its abundant crater Lakes which are supposed to be suitable for palaeoclimate studies because they have small catchment area, with simple basin morphology and rapid sediment accumulation (Lamb *et al.*, 2001; Dramis *et al.*, 2003; Mohammed *et al.*, 2004). The various palaeoclimate proxy data obtained from Lakes include sedimentological records of outcropping lacustrine sequences and ancient shorelines, sediment cores from the Lake bottom, diatom data (species and abundance variations), stable isotope data from authigenic calcite, and pollen data from core samples (Lamb *et al.*, 1999; Lamb *et al.*, 2001; Dramis *et al.*, 2003; Mohammed *et al.*, 2004; Shutt and Busert *et al.*, 2004). Carbon and oxygen isotopes are the most widely used palaeoclimate proxies in

lacustrine sediments and authigenic carbonates precipitated out of Lake water. The  $\delta^{18}\text{O}$  composition of authigenic carbonate precipitated in equilibrium with Lake water is related to the isotopic composition and temperature of Lake water at the time of precipitation and, can be used to track past changes in precipitation: evaporation ratio (P/E). In Lakes with no surface outlet, the  $\delta^{18}\text{O}$  composition of Lake water depends on the balance between isotopic composition of inputs (including the source and amount of precipitation, surface runoff and groundwater inflow) and outputs (evaporation and groundwater loss) (Lamb *et al.*, 2000). Especially in arid and semi-arid regions the dominant control on Lake water  $\delta^{18}\text{O}$  is evaporative fractionation, controlled by temperature and humidity. Nevertheless, annual temperature range in the rift region are small, hence the effect of temperature on the isotopic composition of carbonate precipitation is usually negligible. Additionally the effects of varying precipitation source on  $\delta^{18}\text{O}$  will also be small in comparison to evaporative concentration (Lamb *et al.*, 1999; Lamb *et al.*, 2000, 2006). Provided there is no change in carbonate mineralogy, change in  $\delta^{18}\text{O}$  is often linked to change in P/E. The  $\delta^{13}\text{C}$  value of carbonate is a reflection of the isotopic composition of the total dissolved inorganic carbon pool (TDIC), which largely depends upon photosynthetic activity and exchange with atmospheric  $\text{CO}_2$  (Lamb *et al.*, 2000). Aquatic photosynthesis selectively removes  $^{12}\text{C}$  from the Lake TDIC, so precipitating carbonates have higher  $\delta^{13}\text{C}$  values. Higher  $\delta^{13}\text{C}_{\text{TDIC}}$  values will also occur due to  $\text{CO}_2$  exchange between the Lake TDIC and the atmosphere, a process that becomes more important as water residence time increases. This process will become less important if the Lake is supersaturated with  $\text{CO}_2$ , but the subsequent degassing of  $\text{CO}_2$  from the Lake will also increase  $\delta^{13}\text{C}$  (Lamb *et al.*, 1999; Lamb *et al.*, 2000; 2006). In general, palaeoclimatic information recovered from Lake records (especially crater Lakes in tectonically active regions) need careful understanding of the influence of non climatic influences like hydrothermal influences and groundwater exchange. Hence, replicate records are needed for justification from several sites implying the importance of multi- proxy or multiple indicator approach. According to Henry F. Lamb, 2000, the high resolution isotopic records recovered from the core sediments from crater Lakes (e.g. Tilo and Hora) can contribute to a better understanding of the range and frequency of climate extremes and the nature of rainfall variability at a timescale relevant to the local problems in Ethiopia, a country that is vulnerable to climatic extremes.

## 2.5 Holocene Palaeoclimate of Ethiopia

Holocene Climate (the period 10Kyr to date) in Ethiopia and the region of east Africa is characterized by a general trend of cyclicity between dry and wet conditions (Lamb *et al.*, 1999, 2000; Lamb *et al.*, 2004; Mohamed *et al.*, 2004; Asrat *et al.*, 2007; Baker *et al.*, 2007). Most of the evidences about Holocene climate variability arise from the Lake records in the Main Ethiopian Rift and recent researches showed speleothem records as powerful tools in this regard.

During the early Holocene, the region of east Africa, including Ethiopia was considerably wetter than today (Lamb *et al.*, 2000; Lamb *et al.*, 2002; Mohammed *et al.*, 2004). A good example is the Holocene record of Lake level variability from the Ziway-Shala Lakes in the Main Ethiopian Rift. Gillespie *et al.*, 1983, cited in Lamb *et al.*, 2002; Mohammed *et al.*, 2004, showed that the two Lakes merged to form a single palaeolake between ~10.7-9.5Kyr and from ~6.3-5.1Kyr, when the shore line is estimated to have been approximately 112m higher than the present level of Lake Shala (Lamb *et al.*, 2001, 2006; Lamb *et al.*, 2002; Mohammed *et al.*, 2004). However, this warm period was interrupted by a brief period of aridity between ~8.7-8.1Kyr and at ~6.7Kyr, followed by a major and rapid decline in Lake level after ~5.7-5.1Kyr. Fluctuations of moderate amplitude have been recorded during Late Holocene. A rise of 42m above the present day Lake Shalla level was recorded around 1.9-1.4Kyr and a rise of 70m was dated between 3.8-1.6Kyr. According to Street 1979b, cited in Mohammed *et al.*, 2004, mean annual precipitation in the early Holocene was 28-47% higher than modern rainfall in the Ziway-Shalla Basin. (Lamb *et al.*, 2002; Mohammed *et al.*, 2004). The data recovered from Lake level variations is also supported by other proxies like isotopic records of Lake sediments (Henry F. Lamb *et al.*, 2000; A. Lamb *et al.*, 2003) Pollen data (Lamb *et al.*, 2001) and vegetation variation (Lamb *et al.*, 2001) in the Holocene.

Lamb, 2000 has interpreted the lower oxygen isotope value of a sample from Lake Tilo core that, until early-mid Holocene ~6.3Kyr, a wet climate condition dominated showing higher amount of precipitation than today. This wet condition was interrupted at around ~8.8-8.5Kyr and at 6.7Kyr. An abrupt increase in the oxygen isotope value at 4.7Kyr shows abrupt fall in P/E which was maintained until 4.1Kyr. Over the last 2.6Kyr, the isotopic records from the core of Lake Tilo showed a complex trend of variability. The isotopic records of the Lake Tilo core are

in a good agreement with the Lake level records of the Ziway-Shala Lakes (Lamb *et al.*, 2000; Mohammed et al., 2004 and references there in).

Lamb, 2001 interpreted the pollen record of a sample from Lake Tilo core, in south central rift valley, pointing out that despite the Lake level evidence for strong variations in the moisture regime, the dominance of pollen of savanna vegetation is characteristic of marked rainfall seasonality.

## **Chapter 3: Site description and methodology**

### **3.1 Location**

In this study, the stalagmite samples were collected from the Mechara cave site in south east Ethiopia, and the data for the Lake records was collected from four Lakes from south, central and northern Ethiopia. Detailed description for location of each of the study sites is given as follows.

### **3.2 The Mechara karst area and description of caves**

The Mechara karst area,  $8^{\circ} 30' - 8^{\circ} 45' N$  and  $40^{\circ} 15' - 40^{\circ} 30' E$ , elevation: 1500-1700 m a.s.l. is located 450 Km Southeast of Addis Ababa. The Mechara karst area first discovered in 1995/96 is situated in extensive limestone beds in the Mesozoic sedimentary successions at the southeastern margin of the Main Ethiopian Rift (MER). There are seven major cave systems in the Mechara karst area with sixteen entrances. High resolution speleothem samples suitable for palaeoclimate study have been recovered from three of the cave systems; Achere-Ayange, Rukiessa and Bero. All the three caves are accessible and contain actively growing speleothems suitable for monitoring the modern cave microclimate and hydrology (Asrat et al., 2007, 2008; Baker et al., 2007). Detailed description of each of the three caves is given below.

#### **3.2.1 The Achere-Ayange cave system**

The Achere Ayange cave system (37 651075 E, 0951801N, 1534m a.s.l; and 37 651100E, 0952366E, 1550 respectively) comprises of 7.1 Km passage and is known to be the second longest cave system in Ethiopia (Asrat *et al.*, 2008). It is made up of two caves aligned in NE-SW direction. A total of 3830 m passage has been surveyed in Achere and 3300 m in Ayange. The accessible passage in to the caves lies at 20-25 m vertical zone from the surface. The roof of the caves is a mudstone/marl unit where the floor is not exposed and lined with fine dust and bat guano. Rift related tectonics initiated conduit development in to the caves while lithology might have restricted further dissolution (Asrat *et al.*, 2008). There are also collapse features showing active tectonics in the past. Currently, the Achere-Ayange cave system is relict, 10 m above the active stream. Twelve stalagmites with basal age ranging from 69,000 to 900 years were samples

from this cave system, which are suitable for high resolution palaeoclimate reconstruction (Asrat *et al.*, 2008).

### **3.2.2 Rukiessa cave system**

This cave system (37 651550 E, 09 51300 N, elevation 1618 m a.s.l) is located about 1 Km east of the eastern bank of Mechara river and the Burka spring (37 652300 E, 09 53010 N, elevation 1515 m a.s.l). Buna Kerab cave (37 652746 E, 09 52897 N, elevation 1618) is located some 500m away from the Burka spring. The three caves might probably be part of the same extensive cave system and the Burka spring is the point of emergence of the underground stream that drains the Rukiessa cave. The Rukiessa cave system has approximately 1.1 Km surveyed passage and is wet, continuously flushed by seasonal floods. ~25m beneath the surface, lay the Mercury chamber, with 3m x 3m x 1m dimension where some modern stalagmites including Merc-1 collected, which provided a high resolution palaeoclimate record of the last hundred years. Asfa chamber, a third level from the surface approximately 30 m from the surface; is very wet and it contains pool waters actively growing stalactites and non corroded modern stalagmites including Asfa-3, and older ones like Asfa-5 and Asfa-6 (Asrat *et al.*, 2008).

### **3.2.3 The Bero cave system**

Located at 37643926 E, 09 31425 N, elevation 1363 m a.s.l, is a dry relict rift passage with a total length of 300 m. it is a well decorated cave at a cliff intersected by Ejersa river valley. All the entrances of this cave are largely similar to the Achere-Ayange cave system. There are many relict stalagmites at the floor of Bero cave and among this; Bero-1 stalagmite was analyzed to provide a high resolution palaeoclimate record over its growth period in the early to middle Holocene (Asrat *et al.*, 2008)

Table 1: summary of caves in Mechara karst area, modified after Asrat et al., 2008

Cave	Location	Elevation (m a.s.l)	Total surveyed length(m)	Depth(m)	Geology	Stalagmites sampled	Remark
Achere	37 651075 E 09 51801 N	1534	3830	20-25	Roof: Mudstone, marl  Wall: Limestone  Floor: covered with dust, bat guano, rarely reworked basalt cobbles.	Ach_1	Currently relict and, part of the same maze cave network, no physical connection
Ayange	37 651100 E 09 52366 N	1550	3300	20-25			
Rukiessa	37 652300 E 09 53010 N	1618	1100	20-30	Roof/wall: sandy limestone  Floor: allogenic sediments	Merc_1, Asfa_3  Asfa_4, Asfa_5  Asfa_6	Wet, regularly flushed by seasonal floods.
Bero	37 643926 E 09 31425 N	1363	~ 300		-	Bero_1	Dry, relict

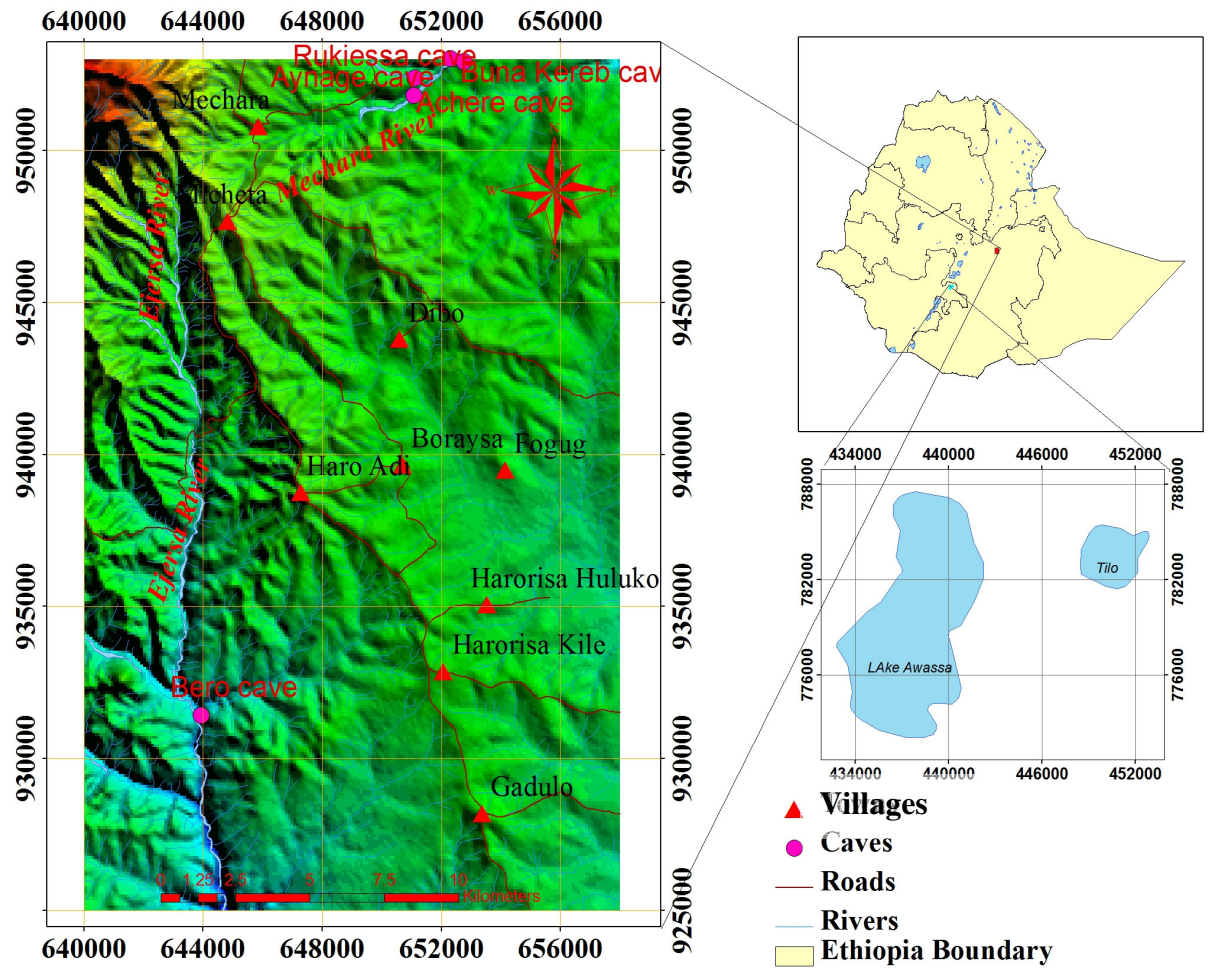


Figure 2: Location map of study sites

### 3.3 Geological Setting

The Mechara karst area is situated in extensive limestone beds in the Mesozoic sedimentary successions at the southeastern margin of the Main Ethiopian Rift (MER) overlain by Oligocene flood basalts. The extensive beds of Jurassic limestone, regionally known as the Antalo Limestone Unit (Asrat *et al.*, 2007), is locally subdivided into the Hamanlei formation, Urandab series and Gabredare series. All the caves in the Mechara karst system have been developed in the Gabredare series. The Antalo Limestone unit with a total estimated thickness of 500-800 m consists of thin, fossiliferous limestone beds intercalated with marl and sandy limestone beds at the top, and massive, crystalline limestone beds intercalated with thin marl and mudstone beds at the bottom (Asrat *et al.*, 2007, 2008). The Antalo Limestone unit is conformably overlain by Jurassic shale (Agula Shale unit) with an estimated thickness of 150m. (Ambaradam Formation) conformably overlies the Agula shale. The Ambaradam Formation, with a total thickness of 100 m, consists of white to pink, medium to coarse-grained, immature, clastic sandstone beds intercalated with silt, shale, mudstone, laterite beds and quartz conglomerates. The Mesozoic succession is affected by fractures and faults with general NE–SW orientation parallel to the rift margin (Asrat *et al.*, 2007, 2008). Most of the karst systems are NE–SW aligned rift passages. The alignment of the caves parallel to the East African Rift system suggests that rift-related extensional tectonics have promoted karstification in the area.

### 3.4 Vegetation history

The organic matter preserved in stalagmites have an important potential to reconstruct the regional paleoclimate, environmental and ecosystem change (Blyth *et al.*, 2006). The organic matters preserved in stalagmites include Lipid biomarkers and pollen. The vegetation cover above the cave plays important role in controlling the  $\delta^{13}\text{C}$  and the trace element signals in speleothems (Baker *et al.*, 2007). The Mechara karst area is currently agricultural, and most of the cave entrances are located in cultivated fields dominated by ploughed fields covered mainly with cereals like maize, millet and cash crops like ‘chat’ and coffee (Asrat *et al.*, 2008). There are remnants of earlier wood vegetation which was destroyed by the one of the major agricultural clearances in the 1930’s in the area. There is a residual soil < 1m thick, covering the fields above the cave (Asrat *et al.*, 2008; Baker *et al.*, 2007)

### **3.5 Climate**

The climate of the Southeastern Ethiopian plateau, including the Mechara karst area, is governed by the general pattern of winds and pressure over the African continent, strongly modulated by topography and the proximity of the Indian Ocean (Asrat *et al.*, 2007). The region is subject to the seasonal migration of the Inter-Tropical Convergence Zone (ITCZ) and is very sensitive to monsoon variability, almost all the rainfall being ultimately derived from the Indian and Atlantic Oceans (Asrat *et al.*, 2007 and references therein). Locally, the area is characterized by an average annual temperature of 23°C and total annual rainfall of 1000 mm having bimodal nature. Recent survey of the cave microclimate conducted in the area shows that temperature is generally constant, while precipitation shows strong seasonal variation where the main rainy season extends from July to September ('big rains') and the 'little rains' fall between March and May (Asrat *et al.*, 2007, 2008). Within cave temperatures in Mechara reflect the total annual surface air temperature (between 20 and 22°C, depending on altitude), while humidity varies between 80% and 100% (depending on the presence of cave streams or drip waters).

### **3.6 Lake sites**

#### **3.6.1 Lakes Tilo and lake Awasa**

Lake Tilo (7°03'45''N, 38°05'45''E; elev. 1545 m a.s.l) is one of three crater Lakes located 40 km southwest of Lake Shala and 40 km west of Lake Awassa. The Lake currently has a surface area of 64 ha and a maximum depth of 11 m. it is currently a saline alkaline Lake with precipitation and local groundwater being the major sources of water input (Lamb *et al.*, 2000) with total annual precipitation of 850 mm, and total annual temperature of 21°C. Relative humidity near the Lake surface varies between 80 and 100% .The region has a semi-arid climate with distinct seasonality influenced by Indian Ocean air flow and the ITCZ.

Lake Awasa (7° 06' N 38° 33') is located in southern part of the main Ethiopian rift at an elevation of 1680 m (Fig.2.). It lies between Ziway-Shala Lakes to the north and Lakes Chamo and Abaya. It lies in a caldera complex with 1300 Km<sup>2</sup> closed basin. The Lake has a total surface area of 92Km<sup>2</sup> and average depth of 10m.

### 3.7 Methodology

This work starts with a detailed literature review regarding speleothem and Lake Palaeoclimate reconstruction of the Holocene in Ethiopia. Collection, systematization and synthesis of all palaeoclimate proxy data from published and unpublished secondary sources on stalagmite and lake archives over the Holocene will be done As discussed in Asrat *et al.*, (2007, 2008); Baker *et al.*, (2007) various lake records from the Ethiopian rift system will be used as a reference in this work. All the four stalagmite samples, Ach-1, Asfa-3, Merc-1 and Bero-1, used in this work were sampled from the Mechara karst area in southeast Ethiopia in the year 2004. Standard procedures were followed to recover relevant palaeoclimate data recorded in the stalagmites as discussed below (Lamb *et al.*, 2000; Mohammed *et al.*, 2004; Fairchild *et al.*, 2006a; Asrat *et al.*, 2007, 2008; Baker *et al.*, 2007).

Stalagmites are usually studied in polished slabs, perpendicular to the direction of the maximum growth. One half of each of the stalagmite samples was polished for lamina counting conducted on the scanned high-resolution images of the polished surface using image processing software (Image Pro Plus 5.0.) The image was enhanced by stretching to full range of pixels (0-255). Lamina width was calculated by measuring the average distance between visible laminae using a 50-pixel wide transect. After laminae counting, the sample was used for geochemical analysis. Analysis of stable isotope records of all the five stalagmites was carried out at the NERC Isotope Geosciences Laboratory at Keyworth (UK).

For Asfa-3 stalagmite, 88 samples were drilled at a regular interval of 1-3mm along the growth axis and samples for Hendy test were taken horizontally along 4 lines. Similarly, for Merc-1 stalagmite, 91 samples were drilled along the growth axis and at 3 lines laterally for Hendy test. For Ach-1 stalagmite, 209 samples were drilled at a regular interval of 1-2 mm along the growth axis and additional samples were taken laterally at six locations for Hendy test. Bero-1 stalagmite is the longest of all the other stalagmites and a total of 802 samples were drilled along its growth axis. Additional samples were taken laterally along ten lines for Hendy test.

Laboratory analysis was carried out following the standard procedure as stated in Asrat *et al.*, 2007, 2008; Baker *et al.*, 2007. All the calcite samples were reacted with phosphoric acid and cryogenically purified before isotope ratio mass spectrometry (IRMA) using an isocarb plus

Optimas dual inlet mass spectrometer. By comparison with a laboratory marble standard, the sample  $^{18}\text{O}/^{16}\text{O}$  and  $^{13}\text{C}/^{12}\text{C}$  are reported as  $\delta^{18}\text{O}$  and  $\delta^{13}\text{C}$  values in permil (‰) versus VPDB. Analytical precision is less than 0.1 ‰ for the standard marble. Lake sediments used in this work are authigenic calcite deposited in the lake water. Lake cores were drilled to recover the  $\delta^{18}\text{O}$  and  $\delta^{13}\text{C}$  isotopic data according to the standard procedure stated in Lamb et al., 2000; Lamb *et al.*, 2006)

The isotope record of the five stalagmites will be compared with each other to examine the nature of correlation and finally, the stalagmites isotope records are compared with isotope record from the lake cores samples. Statistical analysis will be applied using EXCEL, to see the trends and nature of correlation between the proxy records. The time series of the trends of stable isotopes are prepared.

## Chapter 4: Results and Discussion

### 4.1 Results

#### 4.1.1 Stalagmites

A total of four stalagmite samples were used in this study including Ach-1, Asfa-3, Merc-1 and Bero-1. Two of the stalagmite samples (Asfa-3, Merc-1) are modern and the remaining two (Ach-1 and Bero-1) are of Mid-Early Holocene age.

Ach-1 stalagmite (fig.3) is sampled from the Moenco chamber, 200 m from the entrance of the Achere cave. It is 25 cm long and is a continuously laminated stalagmite. The age of Ach-1 stalagmite is dated at the base at 5202 yrs until it stopped growing at 4700 yr BP. It has no hiatus and contains continuously annually growing laminae for  $443 \pm 8$  years.

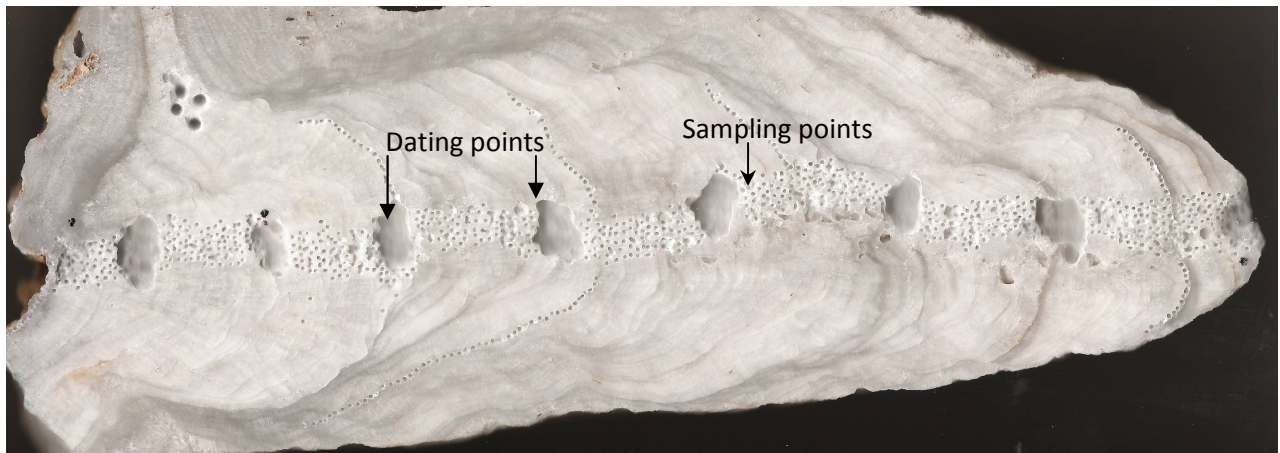


Figure 3: scanned image of Ach-1 Stalagmite

Asfa-3 stalagmite (fig.4) is a modern stalagmite sampled from the Asfa chamber in the Rukiessa cave. It was actively dripping from 1898-2004 while sampled and had continuous visible laminae with no hiatus. The polished surface of the stalagmite exhibits alternating white porous laminae and dark compact laminae with average laminae thickness varying between 0.2-0.4 mm.

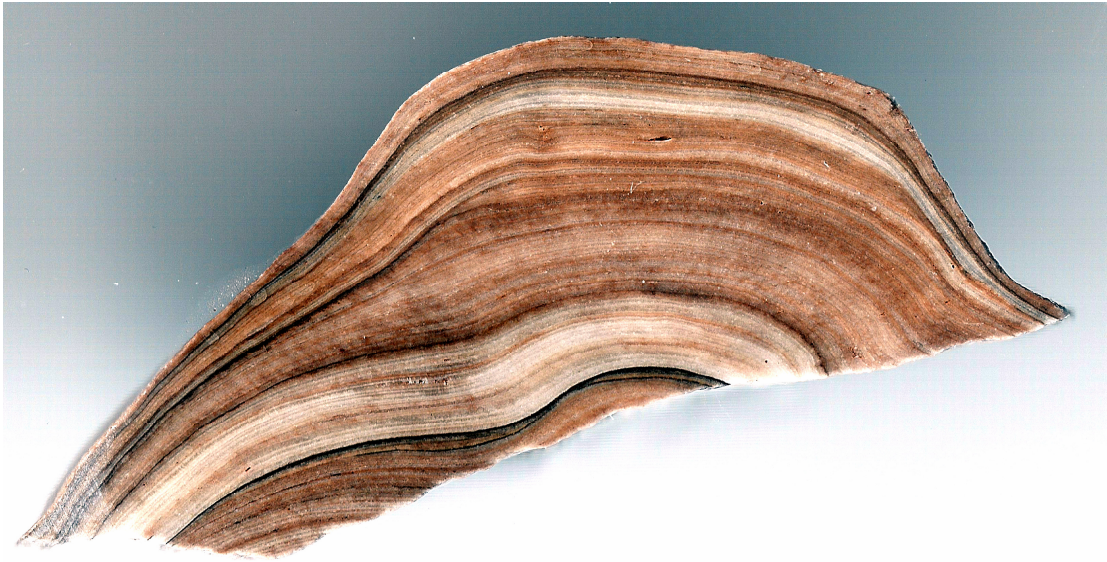


Figure 4: scanned image of Asfa-3 stalagmite

Merc-1 stalagmite has been growing and dated between 1896-2004 years. It is continuously laminated with alternating dark and light laminae with average lamina width of 0.29, and there is no hiatus in the record.

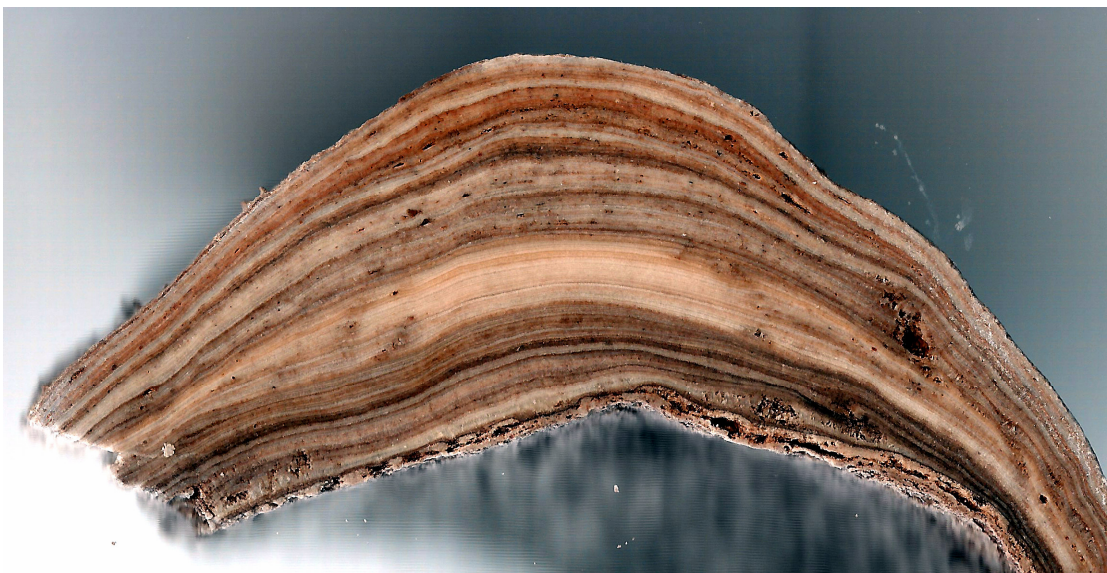


Figure 5: Scanned image of Merc\_1 stalagmite.

Bero-1 stalagmite (fig.5), sampled from the Bero cave, has started growing at 7791 yr BP. (Basal age dated 7791 years at the bottom). It is continuously laminated with alternating dark and light laminae and, because the growth was not continuous, it was interrupted with major hiatuses dated at 45, 4392, 4786, 5 278, 5834 and 7336 years before present. This sample has a total length of 44 cm along its growth axis and is broken in to three pieces during sampling (fig.5).

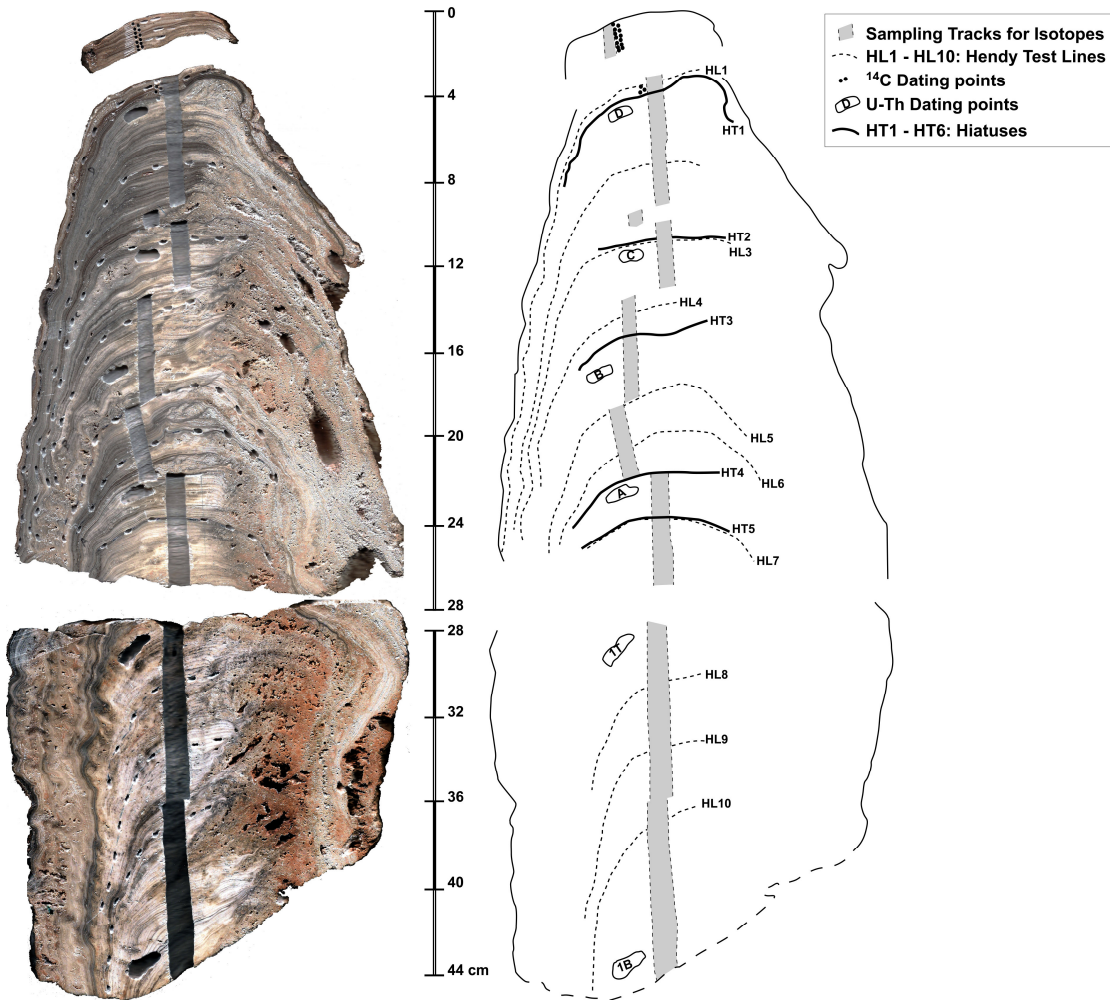


Figure 6: Scanned image of Bero-1 stalagmite (left) and its schematic diagram (right)

## 4.2 Stable Isotopes

### 4.2.1 Asfa-3 Stalagmite

Asfa-3 stalagmite, one of the modern stalagmites collected from the Asfa chamber, has been growing from the 1898-2004. 109 samples analyzed show that the  $\delta^{13}\text{C}$  values show large variation in value, ranging from  $-7.69\text{‰}$  to  $-5.40\text{‰}$ . The  $\delta^{18}\text{O}$  values, with range of values between  $-1.70\text{‰}$  to  $-0.53\text{‰}$ . The  $\delta^{13}\text{C}$  value follows slightly decreasing trend after 1948 while the  $\delta^{18}\text{O}$  value follows nearly constant trend through the growth phase. Between 1930-1976, peak values of  $\delta^{13}\text{C} \sim -5.43\text{‰}$  were recorded around the beginning and end of the growth phases, 1906-1920 and 1990-2004 respectively. Minimum values  $< -7\text{‰}$  were recorded around 1960-1990. For  $\delta^{18}\text{O}$ , peak values  $> -0.75\text{‰}$  were recorded at the beginning of the growth phase, 1907-1927 and minimum values  $< -1.7\text{‰}$  were recorded first at 1899 and around 1930-1960. The two isotopes in Asfa-3 stalagmite show poor correlation with  $R^2=0.0125$ .

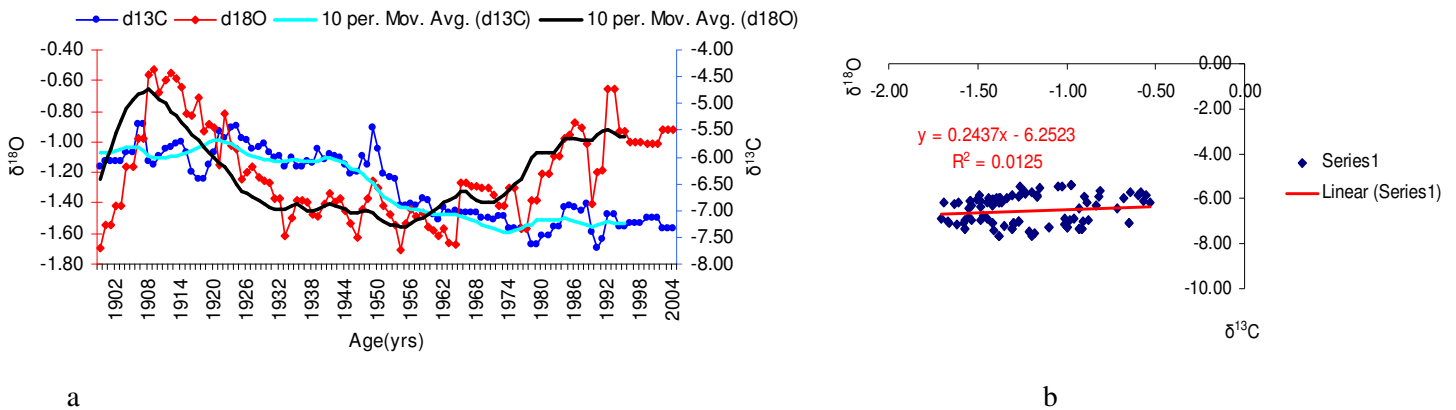


Figure 7: Asfa-3 stalagmite time series (a) and correlation of  $\delta^{18}\text{O}$  Vs  $\delta^{13}\text{C}$  (b)

## 4.2.2 Merc-1 stalagmite

Merc-1 stalagmite has been growing and dated between 1896-2004 years. The mean value trend line of both  $\delta^{13}\text{C}$  and  $\delta^{18}\text{O}$  isotopes show increasing trend through out the growth periods. The  $\delta^{18}\text{O}$  values show wide range of variation from  $-8.1\text{‰}$  to  $-1.64\text{‰}$ , the peak values of  $\delta^{18}\text{O} > -0.5\text{‰}$  were recorded at 1966-1969, 1974-1977 and at 1985, while minimum values  $< -2\text{‰}$  were recorded at 1907, 1924-1927, 1940-1943, 1955, and at 1960-1962. For  $\delta^{13}\text{C}$  isotopes, maximum values  $> -2\text{‰}$  were recorded at 1970, 1981-1983, and at 1988 and minimum values  $< -5.5\text{‰}$  were recorded at 1943, 1953 and at 1979. The two isotopes are generally poorly correlated with  $R^2=0.405$ .

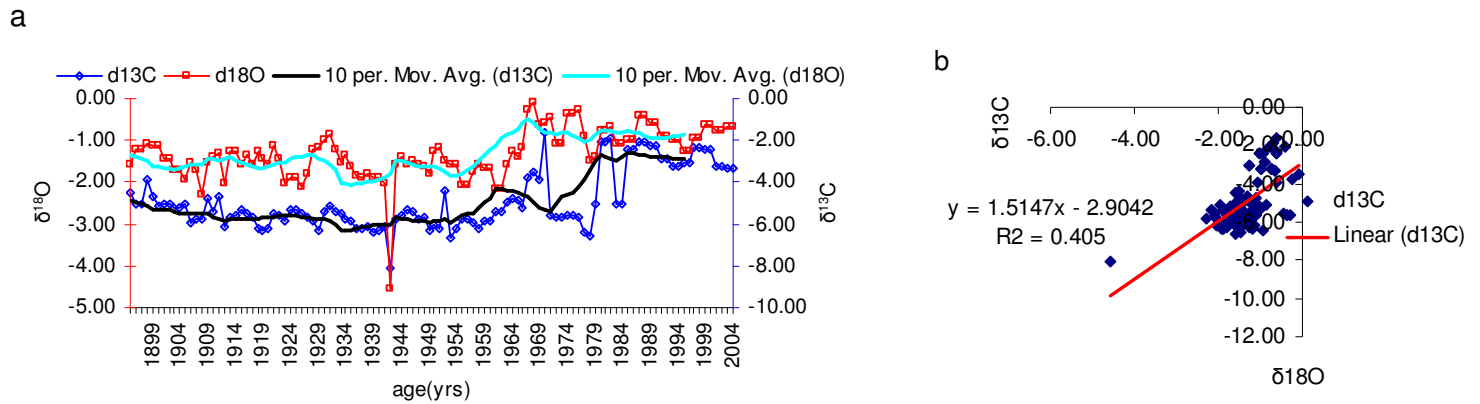


Figure 8: Merc-1 stalagmite time series (a) and correlation of  $\delta^{18}\text{O}$  Vs  $\delta^{13}\text{C}$  (b)

### 4.2.3 Ach-1 stalagmite

Is a continuously growing stalagmite dated between 4700-5202 yr BP. The  $\delta^{13}\text{C}$  and  $\delta^{18}\text{O}$  values analyzed from each of the annual layers show wide range of variation over the growth phase. The  $\delta^{13}\text{C}$  has a maximum value of  $+0.1\text{‰}$  and minimum value of  $-2\text{‰}$  and  $\delta^{18}\text{O}$  has a maximum value of  $-2.4\text{‰}$  and minimum value of  $-4.2\text{‰}$ . Peak values of  $\delta^{13}\text{C} > 0\text{‰}$  were recorded at 4722, 4778-4789 yr BP and minimum values  $< -1.5\text{‰}$  were recorded at 5133, 5150-5170, 5196-5203 yr BP. In the case of  $\delta^{18}\text{O}$ , peak values  $= -2.5\text{‰}$  were recorded at 4723-4725, 5053-5054, 5180-5182, and 5201-5201 yr BP and minimum values  $< -4\text{‰}$  were recorded at 4749-4750, 4813-4814, 4818-4821, 4829-4830. The two isotopes in Ach-1 stalagmite is poorly correlated with  $R^2 = 0.015$ .

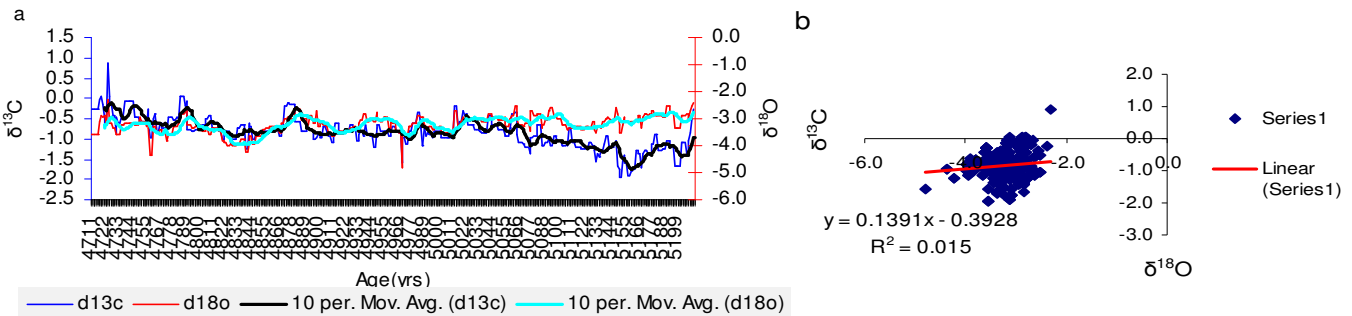


Figure 9: Ach-1 stalagmite time series (a) and correlation of  $\delta^{18}\text{O}$  Vs  $\delta^{13}\text{C}$  (b)

#### 4.2.4 Bero\_1 stalagmite

The  $\delta^{18}\text{O}$  and  $\delta^{13}\text{C}$  value of Bero-1 stalagmite is described in to six different growth phases. There are five major periods of hiatuses (H-1 from 7335-5895 yr BP, H-2 from 5834-5454 yr BP, H-3 from 5277-4865-yr BP, H-4 from 4785-4561 yr BP, and H-5 from 4391-46-yr BP) which are used as a boundary to mark the six growth phases. The time series showing the trend of  $\delta^{18}\text{O}$  and  $\delta^{13}\text{C}$  values of each of the growth phases is described as follows.

Figure 9 bellow shows all the Bero\_1 growth phases A 15 period moving average is made to see the major isotopic trends of Bero\_1 stalagmite in the Holocene and it can be seen that there are five major trends of isotopic variation at an interval of 100-120 years with minor variability ranging from 10-20 years.

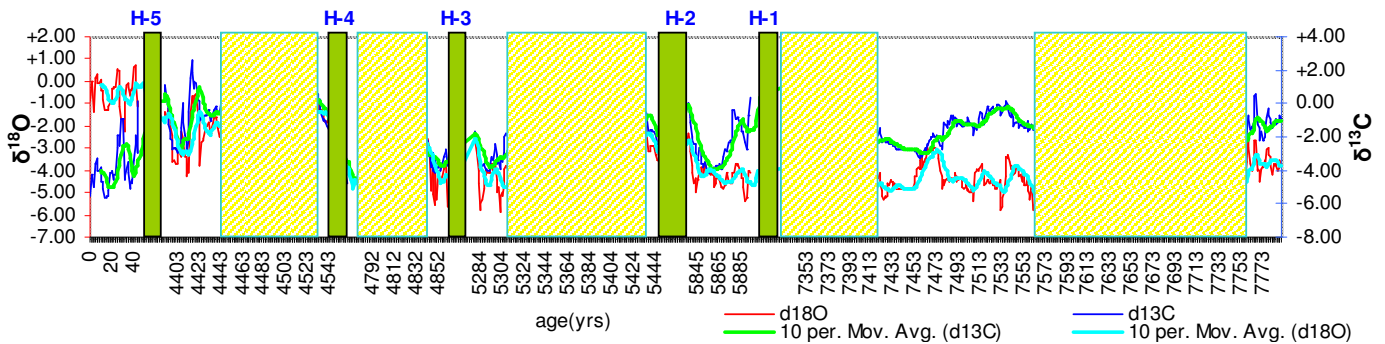


Figure 10: Bero\_1 stalagmite  $\delta^{13}\text{C}$  and  $\delta^{18}\text{O}$  time series, green columns numbered H-1 to H-5 represent hiatuses

### 4.2.5 Bero\_1 growth phase\_1

Growth phase\_1, dated from 7336-7791, is the longest and most continuous growth phase in Bero\_1 stalagmite. Both  $\delta^{13}\text{C}$  and  $\delta^{18}\text{O}$  show very large swing in values, 2.10‰ to -3.25‰ for  $\delta^{13}\text{C}$  and -0.58‰ to -7.49‰ for  $\delta^{18}\text{O}$ . The mean  $\delta^{13}\text{C}$  and  $\delta^{18}\text{O}$  values show a slightly increasing trend towards the top. Peak values of  $\delta^{18}\text{O} > -1.3\text{‰}$  occur at around 7366-7371 and, 7648-7650 yr BP and minimum values up to  $< -7.3\text{‰}$  occur at 7563 - 7338 yr BP. For  $\delta^{18}\text{O}$ , peak values up to  $> +1\text{‰}$  were recorded at 7346- 7880, 7640-7680yr BP and minimum values of  $< -3\text{‰}$  were recorded at 7389-7453, 7486-7565 yr BP. The two isotopes in growth phase\_1 show poor correlation with  $R^2=0.428$ .

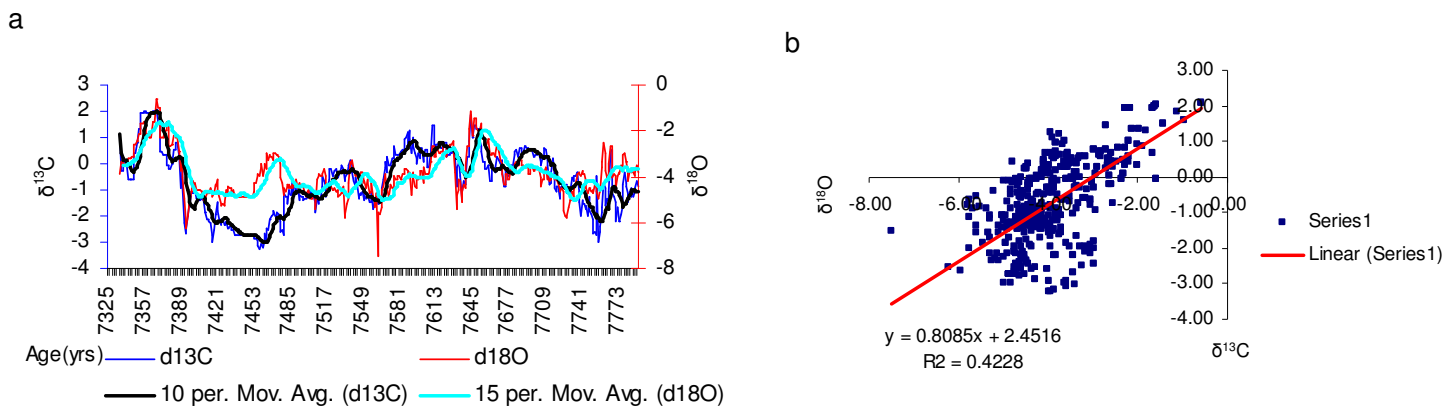


Figure 11: Bero\_1 growth phase\_1 time series (a) and correlation of  $\delta^{18}\text{O}$  Vs  $\delta^{13}\text{C}$  (b)

### 4.2.6 Bero\_1 Growth Phase\_2

At growth phase\_2, between 5835-5894 yr BP, the mean value of  $\delta^{13}\text{C}$  shows generally decreasing trend while the  $\delta^{18}\text{O}$  value follows an increasing trend towards the top. The  $\delta^{13}\text{C}$  value sharply decreases from +0.32‰ to -3.5‰ between 5834-5844 yr BP, It then decreases to -2.9‰ at around 5870 up to 5850. The  $\delta^{18}\text{O}$  gently rises from a minimum value of -5.4‰ at 5889-5891 yr BP to a peak value -2.34‰ at the end of the growth phase. The two isotopes in growth phase\_2 are generally poorly correlated with  $R^2=0.245$

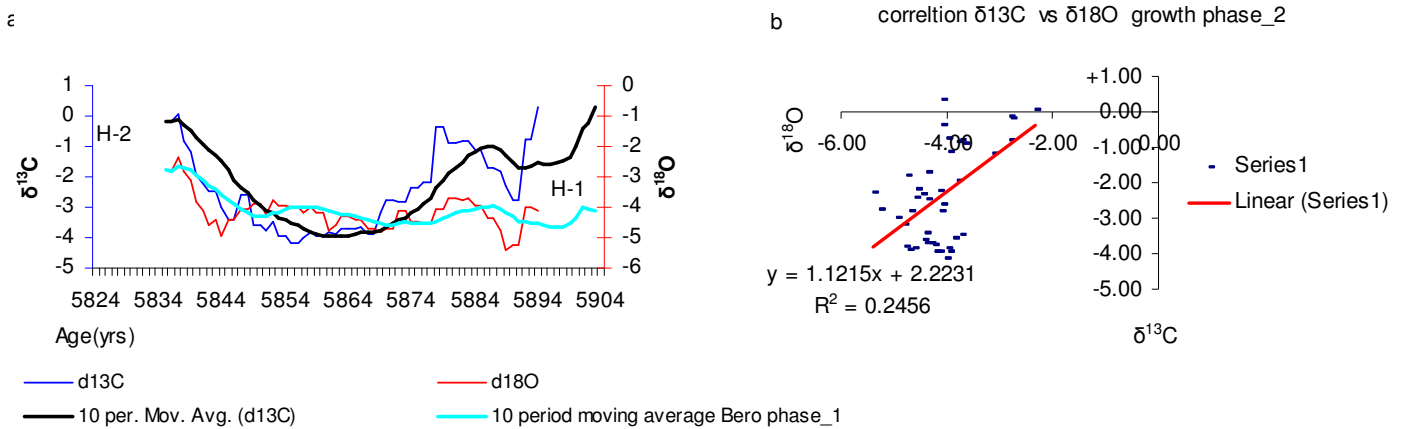


Figure 12: Bero\_1 growth phase\_2 time series (a) and correlation of  $\delta^{18}\text{O}$  Vs  $\delta^{13}\text{C}$  (b)

### 4.2.7 Bero\_1 growth phase\_3

During growth phase\_3, between 5278-5453 yr BP,  $\delta^{18}\text{O}$  has values ranging from  $-0.23\text{‰}$  to  $-5.89\text{‰}$  and the  $\delta^{13}\text{C}$  values range from  $1.81\text{‰}$  to  $-4.09\text{‰}$ . The mean values of both isotopes show decreasing towards the top until the onset of hiatus 3. This growth phase is characterized by a swing of  $\delta^{13}\text{C}$  and  $\delta^{18}\text{O}$  isotopic values where peak  $\delta^{18}\text{O}$  values  $> -1.5\text{‰}$  were recorded around 5380 to 5400 5340-5360, yr BP, and minimum values  $< -5\text{‰}$  were recorded towards the end of this growth phase. In the case of  $\delta^{13}\text{C}$ , peak values  $> +1\text{‰}$  and minimum values  $< -4\text{‰}$  were recorded at the same period to that of the  $\delta^{18}\text{O}$ . The two isotopes generally follow similar trend of variation having good correlation with  $R^2=0.727$

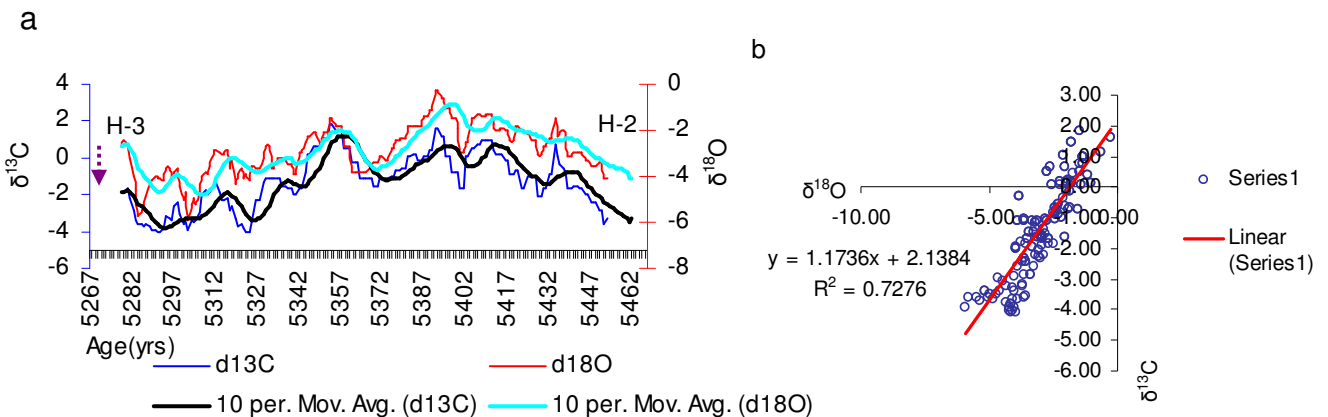


Figure 13: Bero\_1 growth phase\_3 time series (a) and correlation of  $\delta^{18}\text{O}$  Vs  $\delta^{13}\text{C}$  (b)

### 4.2.8 Bero\_1 growth phase\_4

In the fourth growth phase of Bero-1 stalagmite, dated between 4786-4864 yr BP, the mean value of both the  $\delta^{18}\text{O}$  and the  $\delta^{13}\text{C}$  values show an increasing trend towards the top until growth interrupted at 4780 yr BP. There is large variation in  $\delta^{18}\text{O}$  isotopic values ranging from  $-5.61\text{‰}$  to  $-0.11\text{‰}$  and; the  $\delta^{13}\text{C}$  shows a range of values  $-5.04\text{‰}$  to  $+1.11\text{‰}$ . Peak values of  $\delta^{18}\text{O} > -1\text{‰}$  were recorded at 4790-4816 and minimum values  $< -5\text{‰}$  were recorded at 4850-4865. The  $\delta^{13}\text{C}$  values of growth phase\_4 replicates almost the same trend as to that of the  $\delta^{18}\text{O}$  (fig 13) and the peak and minimum values were recorded almost at similar time. The two isotopes generally have very good correlation with  $R^2=0.792$ .

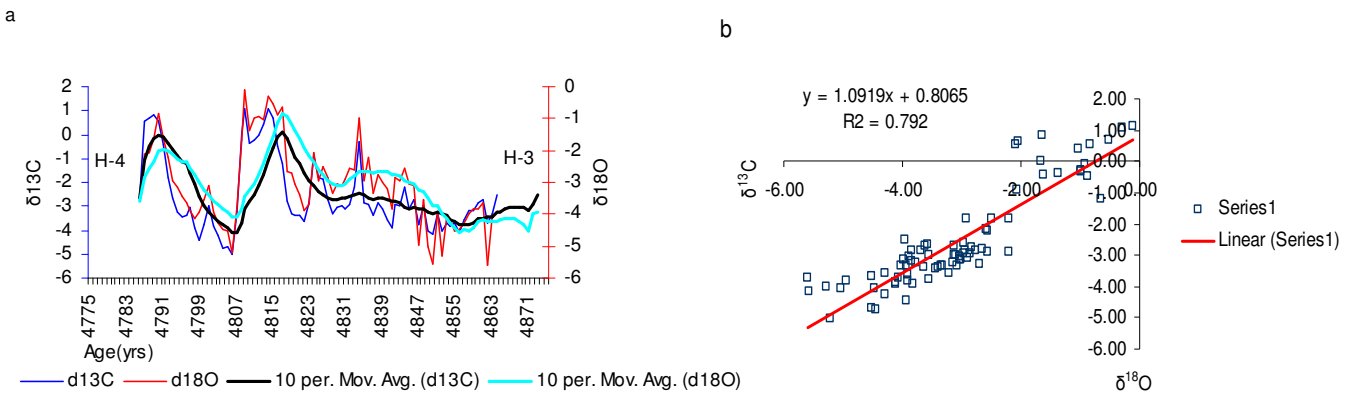


Figure 14: Bero\_1 growth phase\_4 time series (a) and correlation of  $\delta^{18}\text{O}$  Vs  $\delta^{13}\text{C}$  (b)

### 4.2.9 Bero\_1 growth phase\_5

In growth phase\_5, dated between 4392-4560 yr BP, both carbon and oxygen isotopes show very large swing in isotopic value (fig.14). The mean value of  $\delta^{13}\text{C}$  generally shows an increasing trend with a range of values from  $-4.78\text{‰}$  to  $+2.60\text{‰}$  while the  $\delta^{18}\text{O}$  shows a slightly decreasing trend ranging from  $-5.59\text{‰}$  to  $-0.16\text{‰}$  towards the top. The peak value of the  $\delta^{18}\text{O} = -0.16\text{‰}$  is recorded at 4485 to 4540 yr BP and for  $\delta^{13}\text{C}$  the peak value =  $2.60\text{‰}$  is recorded around 4417 yr BP. As can be seen on the graph, there are periods of higher values of  $\delta^{18}\text{O} > -1\text{‰}$  recorded at similar period. Minimum values  $< -4\text{‰}$  were recorded towards the end of the growth phase at 4407 - 4420. The isotopes show generally good correlation with  $R^2 = 0.604$ .

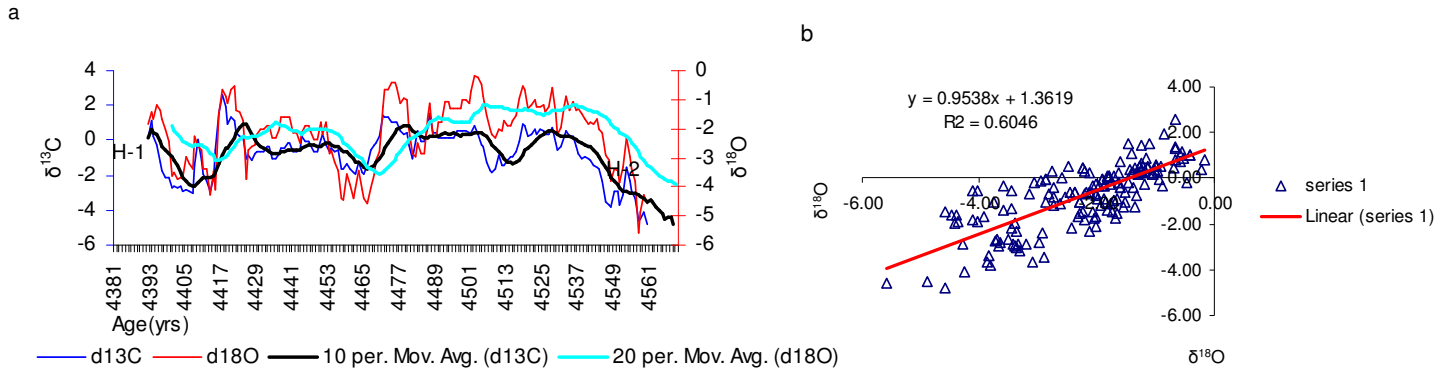


Figure 15: Bero\_1 growth phase\_5 time series (a) and correlation of  $\delta^{18}\text{O}$  Vs  $\delta^{13}\text{C}$  (b)

#### 4.2.10 Bero\_1growth phase\_6

Dated 0-45 yr BP, the  $\delta^{18}\text{O}$  value of growth phase\_6 varies from  $-2.26\text{‰}$  to  $+0.72\text{‰}$  and the  $\delta^{13}\text{C}$  value ranges from  $-5.60\text{‰}$  to  $+0.11\text{‰}$ . As shown in figure 9, the  $\delta^{18}\text{O}$  value generally follows very slightly decreasing trend while  $\delta^{13}\text{C}$  follows increasing trend over growth phase towards the top. Sharp changes in the  $\delta^{18}\text{O}$  values ( $-2.3\text{‰}$  to  $+2.6\text{‰}$ ) are recorded at 25-31. Generally, the  $\delta^{13}\text{C}$  and  $\delta^{18}\text{O}$  show very poor correlation in growth phase\_6 with  $R^2=0.0124$ .

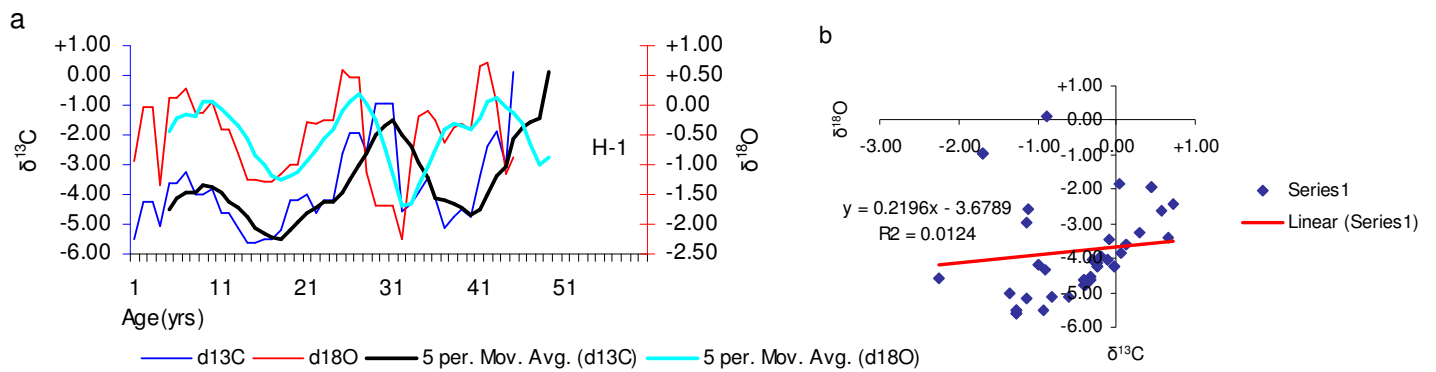


Figure 16: Bero\_1 growth phase\_6 time series (a) and correlation of  $\delta^{18}\text{O}$  Vs  $\delta^{13}\text{C}$  (b)

### 4.3 Brro\_1 Lamina width

Bero\_1 stalagmite has a total of 989 counted lamina from bottom to top. The lamina width varies from a maximum value of 1.40 mm to a minimum of 0.13 mm with an average value of 0.45 mm. The laminae in Bero\_1 stalagmite are annual because the stalagmite is from an area with strong climate seasonality and in addition, the number of lamina is equal to the number of years between two dated points. The laminae show alternating white/dark calcite layers throughout with natural organic matter rich layers and hiatuses through the growth phases. The lamina width of Bero\_1 stalagmite changes almost in an opposite manner through out the Holocene (fig. 16). During the early Holocene, until 7320 yr BP, the lamina width varies in a way that it lowers to a minimum value of < 0.25mm while the  $\delta^{18}\text{O}$  value reaches a peak around 7650 and 7340 yr BP. During the middle Holocene, the  $\delta^{18}\text{O}$  value gently rises and reaches a peak around value of 1.20‰ at 5390 yr BP, and oppositely, the lamina width decreased to a minimum value < 0.25 at the same time. Similarly, in the early Holocene, the lamina width and  $\delta^{18}\text{O}$  continued to vary in an opposite manner. Unlike the  $\delta^{18}\text{O}$ , the lamina width of Bero\_1 stalagmite is characterized by a large swing of values ranging from 1.40-0.13mm. But, the general trend varies along a constant mean value of 0.45mm while the  $\delta^{18}\text{O}$  follows an increasing trend from early to late Holocene. The two records are generally poorly correlated with  $R^2$  ranging from 0.002 to 0.199.

Stalagmite lamina width is affected by cave air  $\text{P}_{\text{CO}_2}$  drip water  $\text{Ca}^{2+}$  content, dip water temperature, and drip water supply rate all of which are affected by surface precipitation conditions (Asrat et al., 2007; Baker et al., 2007). According to Asrat et al., 2008, monitoring of the Mechara caves over a period of 5 years showed constant cave air temperature, and surface and groundwater geochemistry shows similarity through out the area. This shows the lamina thickness of Bero\_1 stalagmite is affected more by the variation of amount of precipitation.

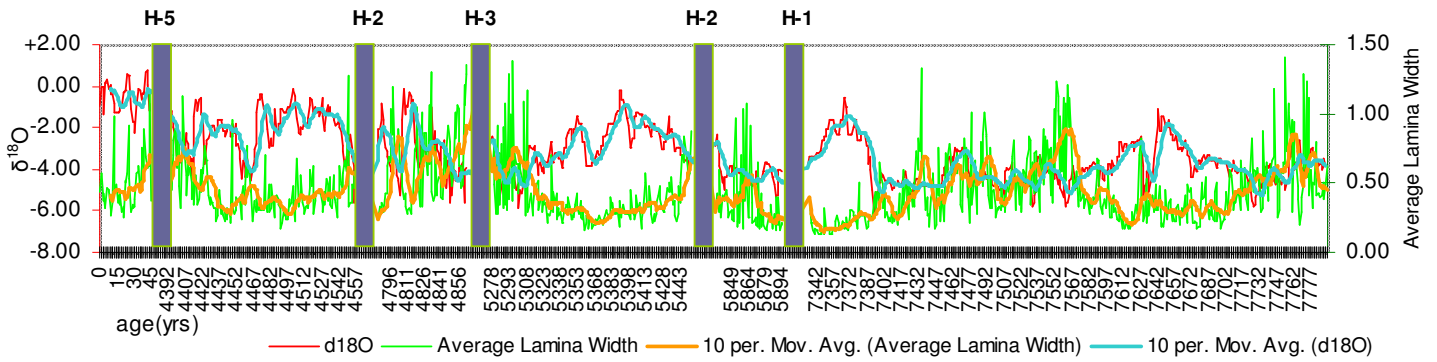


Figure 17: Bero\_1stalagmits Lamina width against  $\delta^{18}\text{O}$ , showing lamina width response oppositely with  $\delta^{18}\text{O}$ ; Blue bars H-1 to H-5, represent hiatuses.

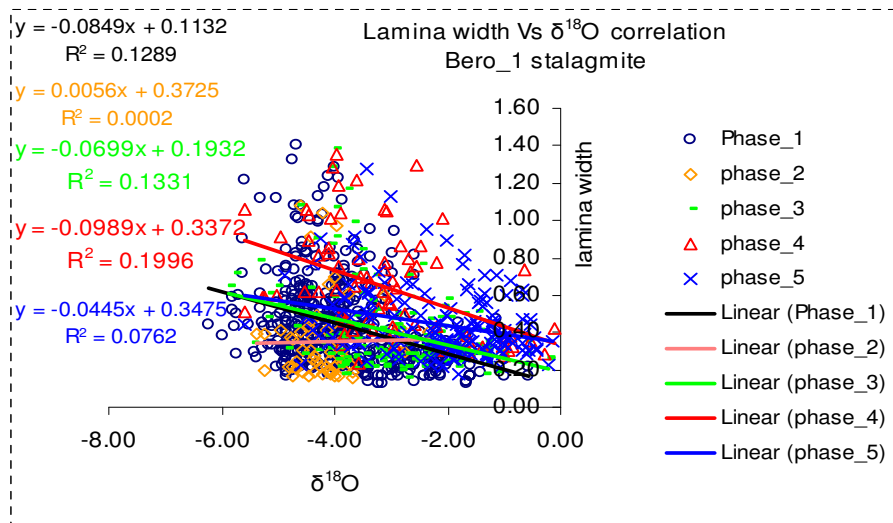


Figure 18: Bero\_1stalagmits Lamina width Vs  $\delta^{18}\text{O}$  correlation of Bero\_1 growth phases 1-6.

#### 4.4 Hiatuses

There are periods of major growth discontinuity recorded especially in Bero\_1 stalagmite. There are a total of five major hiatuses/gaps of stalagmite calcite deposition (fig. 18) from 46-4391 years, 4561-4785 years, 4865-577 years, 5454-5834 years, and finally 5895-7335 years. Some of the hiatuses are as long as 4355 years. Some of the hiatuses fall within the dark laminae, at 4, 11 and 24cm distances from the top of the stalagmite respectively. There are many causes of hiatuses during the growth period of a stalagmite. The hiatus could result from complete cessation in drip source due to extreme dry condition or due to rerouting of the drip source due to seismic disturbances. Usually, hiatuses due to dry events are characterized by presence of detrital dust on the hiatus surface. On the other hand, extreme precipitation could also cause hiatuses due to flooding of the stalagmite surface. In this case, the hiatus surface is covered with dark detrital organic matter, and in cases of huge flooding, corrosion surfaces will be seen (Fairchild et al., 2006).

Hiatus-5, at 4cm from the top of the stalagmite, spans for 4345 years. It is covered with relatively very thick dark layer. The  $\delta^{18}\text{O}$  value at the two ends of the hiatus show relatively enriched values= -1.82 ‰ right at the beginning. The enriched isotopic value may be part of the end of the mid Holocene dry episode around 4414 yr BP. The dark lamina deposited in this period of long hiatus would probably be detrital dust. The recent growth of Bero\_1 stalagmite is restarted before 45 years, which may be due to reopening of drip source routes triggered by a recorded earth quake at 1960-61 nearby Mechara (Asrat et al., 2008). Hiatus-4 is characterized by lower content of dark organic matter. The  $\delta^{18}\text{O}$  value before the beginning of H-4 in growth phase\_5 is -3.85, relatively depleted. The relatively depleted isotopic value may indicate relatively wet climate and some corrosion openings on the scanned image of the polished surface (fig. 5) may indicate corrosion due to excess drip water.

Hiatus 3 is similarly characterized by its content of dark organic material. The  $\delta^{18}\text{O}$  value before the onset of hiatus 3 (end of growth phase\_3) is relatively depleted  $\sim$  -2.70, while the lamina width increases. This shows hiatus 3 may be the result of heavy precipitation and hence cave flooding. Hiatus 2 starts after following an increase in  $\delta^{18}\text{O}$  value (-5.5‰ to -2.78) shown in the earlier growth phase 5. The lamina thickness at this time shows minimum values (fig 16) which together may indicate the start of hiatus 2 be due to dry climate. Hiatus 1 has more dark organic

matter compared with the other hiatuses. The  $\delta^{18}\text{O}$  values at the onset of this hiatus are depleted, and together with the dark organic matter, it may be the result of wetter climate. The isotopic and lamina width values after hiatus 1 follow generally increasing trend (fig.16) and this hiatus 5 could be the end of the early Holocene wet period.

#### **4.5 Equilibrium Condition**

Hendy test conducted for the stalagmite samples in order to check isotopic equilibrium conditions, and the result showed that the  $\delta^{18}\text{O}$  and  $\delta^{13}\text{C}$  values along all the test lines are positively correlated except the poor correlation between the two isotopes in Hendy test line-1, 3 and 4 of Merc\_1 stalagmite. This is indicative of isotopic disequilibrium in all the stalagmite samples used in this study.

Although their positive correlation with the  $\delta^{13}\text{C}$ , the  $\delta^{18}\text{O}$  value along the Hendy test lines in Asfa\_3, and Merc\_1 stalagmites do not show increasing trend. In the case of Bero\_1 stalagmite, the  $\delta^{18}\text{O}$  values show decreasing trend except along Hendy test line-1 with increasing trend.

In addition to the traditional Hendy test, a more reliable test for equilibrium condition is the replication test. When we compare the isotopic values of the stalagmites within the same growth period in similar environment, it is evident that they are not recording the same isotopic values. This is an indicator of other vadose zone alterations that affect the water residence time and amount of dissolved ion concentrations of the water before reaching the cave passage.

Cave monitoring starting from 2004 (Baker et al., 2007; Asrat et al., 2008) showed the relative humidity in most of the Mechara caves in the upper limit of 95%, and most of the caves showed nearly constant temperature variation which supports the minimal evaporative effect. Although stalagmite surface evaporation and rapid  $\text{CO}_2$  degassing are the two possible factors causing isotopic disequilibria, it can be seen that rapid  $\text{CO}_2$  degassing will be the dominant factor. In addition, modern day drip water dissolved calcium concentration and stalagmite growth rate are both higher showing the possible effect of rapid  $\text{CO}_2$  degassing on the isotopic disequilibrium.

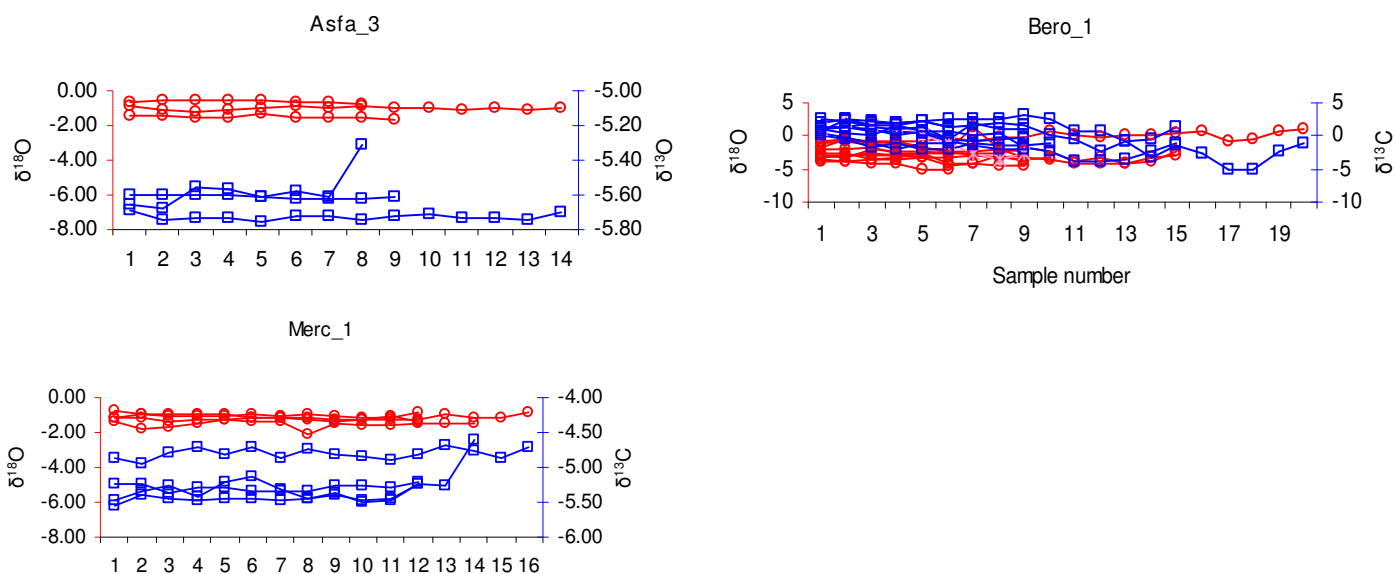


Figure 19: Hendy tests for Asfa\_3, Asfa\_4, Merc\_1 and Bero\_1 stalagmites

#### 4.6 Lake Tilo Core

Lake Tilo core has one of the longest continuous and high resolution stable isotope records recovered from lake sediments. There are seven points where  $C^{14}$  dating is conducted (Lamb et al., 1999) and calibrated in to calendar years. The rate of sedimentation is used together with the age-depth curve (Lamb et al., 2000) in order to determine the age of points in between the actually dated ones. The isotope trend of Lake Tilo in the early Holocene (fig 19) initially start with relatively depleted values  $< -2.5\text{‰}$  until middle Holocene, around 6400 yr BP. The  $\delta^{18}\text{O}$  value gently rises to a peak value  $\sim +4\text{‰}$  around 4000 yr BP and gradually returns back to a lower value  $\sim -2\text{‰}$  around 2600 yr BP after an abrupt fall  $\sim -1\text{‰}$  at 3500yr BP. The  $\delta^{18}\text{O}$  value of Lake Tilo core shows high frequency and high amplitude changes (ranging from  $+6\text{‰}$  to  $-10\text{‰}$ ), after 2400yr BP and finally reaches to a peak value of  $+8\text{‰}$  very recently in the late Holocene. (Fig19). Assuming the isotopic composition of the precipitation source did not change and the surface temperature of the lake area to be  $25^{\circ}\text{C}$ , the isotopic composition of the lake water from which the authigenic calcite has precipitated in the early Holocene will be  $\sim 1\text{‰}$  (Based on O'Nel's formula)

$$T\text{ }^{\circ}\text{C} = 15.7 - 4.36 (\delta^{18}\text{O}_c - \delta^{13}\text{C}_w) + 0.12 (\delta^{18}\text{O}_c - \delta^{13}\text{C}_w)^2 \dots\dots\dots\text{O'Neil et al., 1996}$$

This value is more depleted than the current  $\delta^{18}\text{O}$  value of lake Tilo  $\sim +8\%$ .

Depleted isotopic values (lower  $\delta^{18}\text{O}$ ) in lake sediments reflect relatively humid condition with low evaporation, and enriched isotopic values (higher  $\delta^{18}\text{O}$ ) show relatively dryer/higher E condition with greater evaporation. Hence, the isotope trend of Lake Tilo core generally reflects a wet condition during early Holocene until 4000yr BP followed by a short dry middle Holocene climate up to 4000yr BP and finally followed by relatively dry late Holocene conditions.

The whole lake Tilo core is subdivided in to three units, TL-1to TL-3, from bottom to top, in order to clearly see the trend of isotopic variation through out the Holocene. Both  $\delta^{13}\text{C}$  and  $\delta^{18}\text{O}$  isotopes in TL-3, unlike units TL-1 and unit TL-2, show low range of variation through out. The mean  $\delta^{18}\text{O}$  value generally follows a decreasing trend and the  $\delta^{13}\text{C}$  value follows slightly increasing trend. The two isotopes in unit TL-1 are poorly correlated with  $R^2=0.102$ . In unit TL-2, from 4225 to 2430 yr BP, the two isotopes initially reach a peak value from 3800 to 4050 yr BP, followed by isotopic depletion around 3700 to 3200 yr BP. It then rises up around 2500 yr BP. Finally, at the top of the core, unit TL-3, the  $\delta^{13}\text{C}$  and  $\delta^{18}\text{O}$  values show very large swing in values. The general isotopic trend in this unit starts with relatively depleted value  $\sim -2.5$  and rises to  $> +2.5$  from 200-100 yr BP and finally starts to decrease towards the top of the core. The  $\delta^{13}\text{C}$  and  $\delta^{18}\text{O}$  value of lake Tilo core is

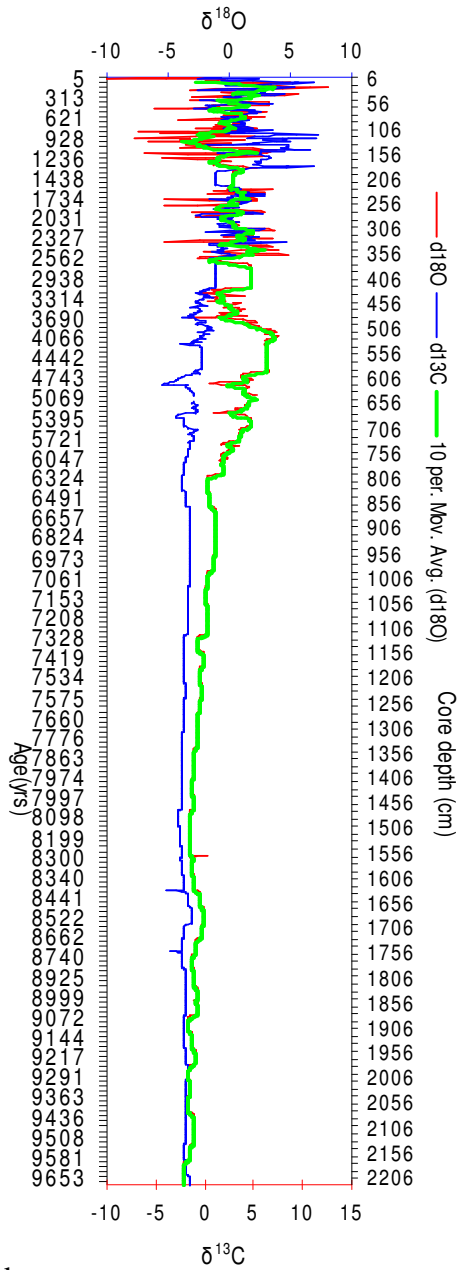


Figure 20: Lake Tilo isotope record

#### 4.7 Lake Awassa core

The Lake Awassa core  $\delta^{18}\text{O}$  values ranging from +7‰ to ~ -1‰. At the bottom of the core; the isotopic value increases from +2‰ to +4‰, followed by a sharp drop of values to -1‰ around 6000yr BP. The relatively depleted isotopic value gradually rises and reaches a maximum value of +7‰ around 4600yr BP (762cm core depth). The enriched isotopic trend around the mid Holocene starts to decrease and finally reaches to ~ +3.5‰ at 3900yr BP (610cm core depth). This relatively depleted isotopic condition continues until interrupted by a short lived sharp fall in  $\delta^{18}\text{O}$  values to ~ 0‰ at 1410yr BP, followed by immediate rise to back to +5.5‰. Finally, the Lake Awassa isotope value continues to increase up to the top of the core with values ~ +7‰. The  $\delta^{13}\text{C}$  value starts with a depleted value around -0.5‰ compared to the  $\delta^{18}\text{O}$ , and then gradually rises to ~ +6‰ at ~4200 yr BP. The  $\delta^{13}\text{C}$  value replicates the trend of the  $\delta^{18}\text{O}$  variation almost through out of the core, but with different magnitudes of variation.

The isotopic trend observed in Lake Awassa core almost exactly agrees with the Holocene Ziway-Shalla lake level fluctuation. The depleted isotopic values at the bottom of the core around 6000yr BP coincides with the early-mid Holocene wet period, with the peak  $\delta^{18}\text{O}$  value around 4600 indicating the mid Holocene dry maximum. The sharp decline in isotopic value around 1410yr BP coincides with the short but largely wet event in the late Holocene that resulted in the rise of Lake Shalla level by 42m (Lamb et al., 2001; Mohammed et al., 2004)

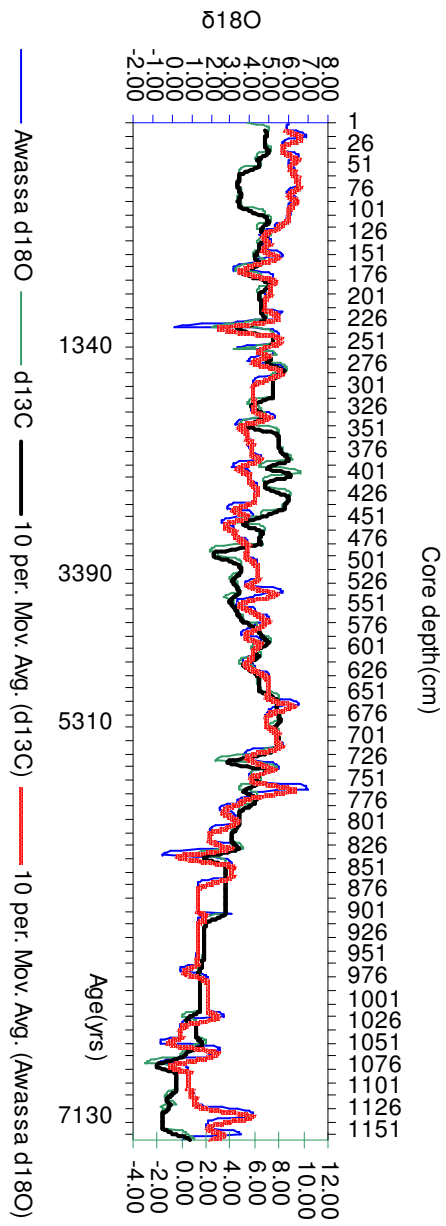


Figure 21: Lake Awassa isotope record

## 4.8 Discussion

Oxygen isotope ( $\delta^{18}\text{O}$ ) variations in speleothem calcite can be indicative of both changes in the cave temperature and changes in the isotopic composition of cave water, which may be climatically controlled and directly related to that of the rain water composition (Bar-Matthews and Ayalon *et al.*, 1997; Mickler *et al.*, 2004). In the case of the Mechara karst area, where mean annual surface temperature shows little variation, the effect of cave temperature on stalagmite isotopic composition is considered to be minimal. Monitoring of cave interior air temperature (Asrat *et al.*, 2008) in the Mechara caves over the period of two years (2005-2007) showed nearly constant temperature of  $18.03^{\circ}\text{C} \pm 0.61^{\circ}\text{C}$  to  $19.47^{\circ}\text{C} \pm 2.93^{\circ}\text{C}$  over the recording period.

Other factors which potentially affect the oxygen isotopic composition of the rainwater and the speleothem calcite, like the rainwater composition effect, the ice volume effect, the amount effect and the effect of evaporation in the vadose zone above the cave could be important in affecting the  $\delta^{18}\text{O}$  of speleothem calcite (Lauritzen and Lundberg., 1999; Araguas *et al.*, 2000; Xia *et al.*, 2001; Williams *et al.*, 2004). The relative importances of these effects depend on the geographic location of the cave and the scale of climate change in the area. Accordingly, the Mechara karst area is located in low latitude tropical region under the influence of monsoon variability (Asrat *et al.*, 2007, 2008; Baker *et al.*, 2007). In this case, the amount effect is the most dominant factor that affects the  $\delta^{18}\text{O}$  value of precipitation such that an increase in the amount of monsoonal precipitation will result in lower/lighter  $\delta^{18}\text{O}$  values while heavier  $\delta^{18}\text{O}$  values correspond to dryer periods (Bar-Matthews *et al.*, 1999; Doralle *et al.*, 2001; Burns *et al.*, 2003; Fleitmann *et al.*, 2003; Mickler *et al.*, 2006; Baker *et al.*, 2007).  $\delta^{18}\text{O}$  values from cave drip and pool waters, springs and rivers in the area fall within Addis Ababa and global meteoric water line (Asrat *et al.*, 2008); showing non equilibrium evaporative processes above the cave surface pose minimal effect on the isotopic composition of the cave drip water and hence, we can deduce that the effect of vadose zone evaporation on speleothem isotopic composition in the Mechara area is minimal.

Based on the above discussion, the  $\delta^{18}\text{O}$  values of the stalagmite samples from the Mechara karst area can be used to reconstruct past climate trends; point out periods of dry and wet climate conditions in the Holocene and compare the stalagmite and lake records in this period.

What makes the Mechara karst system and its stalagmites interesting for the application of palaeoclimate reconstruction is that there are abundant annually laminated stalagmites which can record first order climate signals, i.e. with minimal surface noise (Asrat et al., 2008). Due to the bimodal nature of precipitation in the Mechara area (the small spring rain preceding the big summer rains), the stalagmites isotope signal is more sensitive to the little spring rains, which largely affects the soil moisture and hence the crop productivity and drought conditions than the summer rains. This condition makes the Mechara stalagmites to be of prime interest in understanding the rainfall variability and drought history in Ethiopia (Asrat et al., 2007; Solomon Kassa., 2007).

From the curve showing the  $\delta^{18}\text{O}$  variation of Bero\_1 stalagmite (fig.22.), we can extract five major trends of isotopic cycles in the Holocene between 7800-7500, 7400-7300, 5400-5300, 4860-4800, and 4550-4470 yr BP. According to the earlier discussions, the peak  $\delta^{18}\text{O}$  values observed around 7650, and 7370 yr BP in the early Holocene, 5300-5400, 4801-4860 and 4470-4530 yr BP in the middle Holocene, and the recent late Holocene peak at the end of the growth phase correspond to the relatively reduced moisture/ lower precipitation periods in the Holocene. Similarly, the lower isotopic values between 7590-7450, 5890-5860, 5290-5320 correspond to relatively depleted  $\delta^{18}\text{O}$  values and hence wetter periods.

This interpretation is further supported by observation of change in stalagmite lamina width. The mean annual growth lamina in stalagmites reflect surface climate like the amount of precipitation and drip water supply, drip water  $\text{Ca}^{2+}$  concentration, and drip water temperature. (Frisa et al., 2003, Asrat et al., 2007) Cave monitoring results showed that the drip water amount and variation affects the stalagmite lamina width because the other factors are nearly constant and similar in the Mechara cave area, except variation of precipitation which affects the lamina width in an opposite manner. As can be seen in figure 23, the lamina width of Bero\_1 stalagmite follows a trend opposite to the  $\delta^{18}\text{O}$  variation. A 10 period moving average line is drawn in order to see the major trends of variation over the whole growth phase, and it shows four major phases of variation. It can be seen that the lamina width values clearly decrease as the  $\delta^{18}\text{O}$  values increase and vice versa. Lamina thickness is positively correlated with amount of precipitation, where thicker laminae precipitate during periods of increased amount of drip water related with increased precipitation. As to the previous interpretations, the  $\delta^{18}\text{O}$  trend reflects the variation of amount of precipitation where precipitation amount is inversely related to amount of  $\delta^{18}\text{O}$ .

Hence,  $\delta^{18}\text{O}$  and lamina width trends can be used together to reconstruct variation of precipitation amounts. Based on this discussion, periods around 7650, 7350 yr BP, in the early Holocene, 5380, 4815, 4480 yr BP of the middle Holocene and in the late Holocene where reduced mean lamina width recorded correspond with relatively dryer periods and periods like 7700, 7500, 5850, 5280, 4820 and 4400 where thicker mean lamina width were recorded correspond with relatively more moist and humid periods.

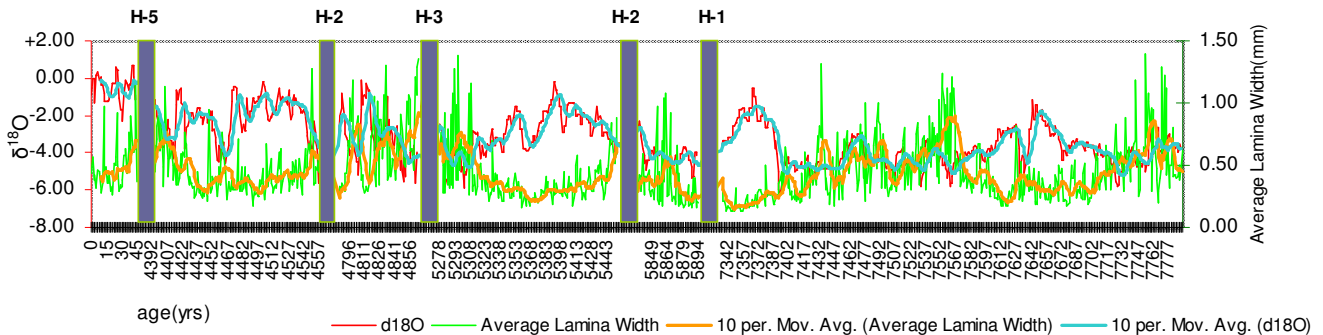


Figure 22: Lamina width Vs  $\delta^{18}\text{O}$ , with the 10 period moving average line of  $\delta^{18}\text{O}$  (green), Lamina width (blue) and growth phases\_1 to 6.

#### 4.9 Comparison of stalagmite Records

Bero\_1, Asfa\_3, and Merc\_1 samples have overlap in last 45 year of growth period, and a comparison made between the  $\delta^{18}\text{O}$  and  $\delta^{13}\text{C}$  values (fig 26) show that the stalagmite records in the Mechara karst area do not show the same trend and amplitude of variation over time. The isotopic trend of Asfa\_3 and Merc\_1 show a generally decreasing trend while Bero\_1 shows nearly constant mean value. All the three stalagmites fall within the range of  $-2.2\text{‰}$  to  $+0.8\text{‰}$ . Asfa\_3 shows the minimum variation of  $\delta^{18}\text{O}$  values between  $-1.70\text{‰}$  to  $-0.53\text{‰}$ . The trends of  $\delta^{18}\text{O}$  record of individual stalagmites show different nature of variation. For example, the  $\delta^{18}\text{O}$  record of Merc\_1 and Bero\_1 stalagmites reflect almost opposite trend between 4-19, 25-33, and 39-44 yr BP. In the case of  $\delta^{13}\text{C}$  values, Merc\_1 shows a decreasing trend and Bero\_1 shows an increasing while that of Asfa\_3 shows almost similar trend through out the initial growth phase. Asfa\_3 and show minimum range of variation  $-5.40\text{‰}$  to  $-7.69\text{‰}$ , similar to the  $\delta^{18}\text{O}$  value, the

$\delta^{13}\text{C}$  value of Bero\_1 and Merc\_1 records show opposite trend of variation and poorly correlated to each other with  $R^2$  for Bero\_1=0.0124, Merc\_1=0.150, Asfa\_3=0.005.

All the isotopic records in the four stalagmites were over the same growth period and from the same climatic region with similar precipitation source. A possible explanation for the different variation in the isotopic trend may be because of variability in the percolation process above the drip source and the variation in the drip route to the individual stalagmites. This shows other hydrological variables in the vadose zone above the cave and through the drip route could influence the isotopic record in the stalagmites. According to baker *et al.*, 2007, Asrat *et al.*, 2008; speleothem isotope records extracted from the same cave may vary because of the variable connection to event water and stored water in the aquifer above the cave.

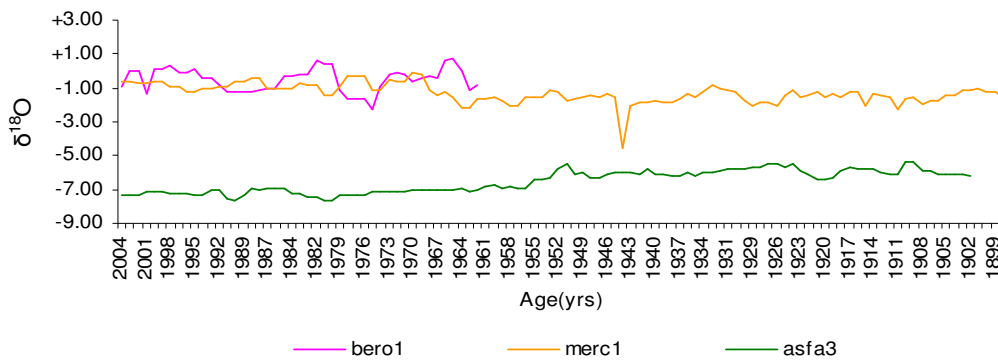


Figure 23: Asfa\_3, Merc\_1 and Bero\_1  $\delta^{18}\text{O}$  and  $\delta^{13}\text{C}$  comparison

## 4.10 Comparison of speleothem Vs lake isotope records

### 4.10.1 Comparison parameters:

The precipitation amount effect is the dominant influencing factor on  $\delta^{18}\text{O}$  value of stalagmites. All the stalagmite samples are grown in humid cave interiors where evaporative effects are minimal. Also, the effect of temperature on the  $\delta^{18}\text{O}$  variation is not significant because the seasonal temperature variation in the region is very small. If the  $\delta^{18}\text{O}$  of speleothem calcite was influenced by temperature, the mean  $\delta^{18}\text{O}$  value of Bero\_1 stalagmite =  $-3.19\text{‰}$  would require around  $13^\circ\text{C}$  annual temperature variation (calculated from the  $-0.24\text{‰}$  fractionation per  $^\circ\text{C}$ , Doralle et al., 2001) ; which is non reasonable in Mechara area with very small seasonal temperature variation(Asrat et al., 2008). In addition, the isotopic values of drip waters in the Mechara caves (Asrat et al., 2008) concentrate around the GMWL with weighted mean annual  $\delta^{18}\text{O} = -0.8$  and  $\delta\text{D} = +4$ . This shows evaporative effect is minimal in the case of drip water  $\delta^{18}\text{O}$  values that reach to the stalagmites. The  $\delta^{18}\text{O}$  of the speleothem calcite precipitated out of drip waters reflects the  $\delta^{18}\text{O}$  signature of the drip water, and hence precipitation, in the time of calcite precipitation. Therefore, the  $\delta^{18}\text{O}$  value of drip water can be derived using the O'Neil's equation

$$T\text{ }^\circ\text{C} = 15.7 - 4.36 (\delta^{18}\text{O}_c - \delta^{18}\text{O}_w) + 0.12 (\delta^{18}\text{O}_c - \delta^{18}\text{O}_w)^2 \dots\dots\dots\text{O'Neil et al., 1996}$$

The  $\delta^{18}\text{O}$  of variation in lake carbonates precipitated in isotopic equilibrium with lake water depends on the isotopic composition and temperature of the lake water during precipitation. In the case of lakes with no surface outlet, (like Lake Tilo and Awassa) it depends on the balance between the isotopic composition of all inputs and outputs (surface and groundwater). But in arid regions, the dominant controlling factor is evaporative enrichment controlled by temperature and humidity. Annual temperature variation is very small; the effect of temperature on isotopic composition of carbonates is minimal. Hence, change in  $\delta^{18}\text{O}$  is often linked to changes in P/E (Lamb et al., 2000). The lake water residence time is important factor, which controls the isotopic enrichment of both  $\delta^{18}\text{O}$  and  $\delta^{13}\text{C}$  by evaporation. Changes in rainfall in the past which may cause lake water residence time to change, is an important controlling factor on the  $\delta^{18}\text{O}$  composition of carbonates in Lake Tilo.

Hence, climate forcing parameters which affect the lake authigenic carbonate  $\delta^{18}\text{O}$  records are different from the climate forcing which affects speleothem isotope records. Modern day isotopic composition of lake Tilo (Lamb et al., 2000) with  $\delta^{18}\text{O}$  average +8.1 and  $\delta\text{D}$  +44 have a gradient of  $\sim 4.5$ , lie off the GMWL showing the lake water is heavily evolved due to the evaporative effect. For stalagmite records, the isotopic values of drip waters in the Mechara caves (Asrat et al., 2008) concentrate around the GMWL with weighted mean annual  $\delta^{18}\text{O} = -0.8$  and  $\delta\text{D} = +4$ . This shows evaporative effect is minimal in the case of stalagmite  $\delta^{18}\text{O}$  values. Hence, the  $\delta^{18}\text{O}$  values of authigenic carbonate from lake sediments are expected to reflect the effect of evaporation and accordingly, period with depleted/lower  $\delta^{18}\text{O}$  values are interpreted as lower evaporation (E) and enhanced precipitation (P)/more humid conditions and higher/enriched  $\delta^{18}\text{O}$  values are interpreted as relatively higher evaporation and lower precipitation conditions.

The  $\delta^{18}\text{O}$  value of authigenic carbonate can be used to calculate the  $\delta^{18}\text{O}$  amount of the lake water during calcite precipitation using O'Neils' equation (O'Neil et al., 1996).

Assuming the surface T °C of the lake water surface is more or less similar to the present day Temperature = 25°C (Lamb et al., 2000), the lake water  $\delta^{18}\text{O}$  value can be calculated.

The  $\delta^{18}\text{O}$  trends of the lake and stalagmite records are compared based on the above discussion that the precipitation amount which is the major controlling factor for speleothem  $\delta^{18}\text{O}$  variation, while the variation in precipitation amount similarly affects the lake P/E ratio, and water residence time and the degree of lake water  $\delta^{18}\text{O}$  enrichment. In this case, periods of reduced precipitation amount (recorded as relatively enriched  $\delta^{18}\text{O}$  in speleothems) will increase lake water residence time and hence, the  $\delta^{18}\text{O}$  record of the authigenic carbonate will show much more enriched values and vice versa.

#### 4.10.2 Bero\_1 stalagmite Vs Lake Tilo isotope record

#### 4.10.3 Bero\_1 growth phase\_1 vs. Unit TL-1

Compared with Bero growth phase\_1; the  $\delta^{18}\text{O}$  value of the lake Tilo core unit TL-1 between 6320-8740 shows a decreasing trend from a minimum value of  $-0.54\text{‰}$  to  $-3.26\text{‰}$ . The  $\delta^{18}\text{O}$  value of Bero growth phase\_1 (from 7789-7325) follows increasing trend until interrupted by a 1440 years long major hiatus (H-1) at 7336yr BP (fig 24) with a value ranging from  $-3.5\text{‰}$  to  $-0.25\text{‰}$ . Because the two climate archives respond at different temporal scale, the small scale  $\delta^{18}\text{O}$  variability at a time scale of 10-20 years that we see in the stalagmite record is not visible in the lake record. Instead, only the major isotope trends are correlated (fig. 24). The  $\delta^{18}\text{O}$  values of lake Tilo core in the early Holocene shows very little variation until 6300 yr BP. This is due to the influence of groundwater inflow in to the lake which has influenced the response of the lake water  $\delta^{18}\text{O}$  to P/E variation and the rate of calcite precipitation (Lamb et al., 2000). The relatively depleted, but gradually rising  $\delta^{18}\text{O}$  value in both Bero\_1 and unit TL-1 core reflect the relatively wet and humid climate in the early-mid Holocene. And the sharp rise in isotopic values of unit TL-1 closer to 6300 years continues until the mid Holocene dry maximum, while part of Bero\_1 stalagmite is not deposited probably due to extreme dry events. The lamina width of the Bero\_1 stalagmite also responds in a way that initially, the mean lamina width decreases to a minimum of  $\sim 0.25\text{mm}$  around 7560, while the  $\delta^{18}\text{O}$  value reaches a peak value  $\sim +1$  in the early Holocene. It rises slightly around 7550 to  $\sim +1\text{mm}$ , and continues to diminishes to  $+0.25$  before the onset of the hiatus H-1 (fig 23). This show, the average lamina width varies responds in an opposite trend to the  $\delta^{18}\text{O}$  value showing that lamina width increases as the precipitation amount increases and decreases as it gets relatively drier.

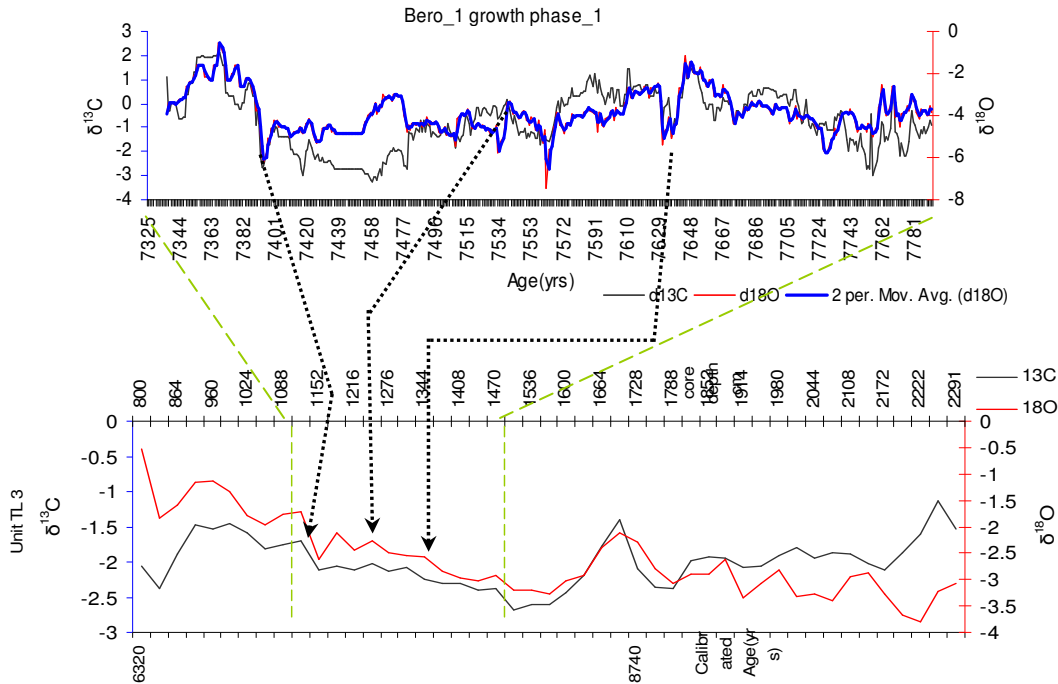


Figure 24: Bero\_1 Vs unit TL-1 comparison

#### 4.10 4 Bero\_1 growth phase\_2, 3, 4, 5 Vs Unit TL-2

Bero growth phase\_2, Phase\_3 and phase\_4, initially start with depleted  $\delta^{18}\text{O}$  value =  $-4.17\text{‰}$  which is relatively more depleted than Phase\_1 (mean  $\delta^{18}\text{O} = -3.84\text{‰}$ ) showing relatively more humid conditions. It then becomes enriched to a mean value of  $-0.29\text{‰}$  around 5400 yr BP in growth phase\_3 and gently depleted to  $\sim -4$  before the hiatus-3. Again, around 4800 yr BP, the  $\delta^{18}\text{O}$  value becomes enriched to  $\sim 0\text{‰}$  but soon followed by sharp reduction to  $-5\text{‰}$  around 4790. Finally between 4557-4400 in growth phase\_5, the  $\delta^{18}\text{O}$  value becomes more enriched to a mean value of  $-2.18\text{‰}$ .

The isotope record in unit TL-2 (2430-6320 yr BP) starts with a relatively depleted value of  $-0.24\text{‰}$  and gently increases to a peak value of  $+3.61\text{‰}$  around 4000 yr BP and then sharply becomes depleted to  $-0.05\text{‰}$  around 3600 yr BP. Abrupt change in the  $\delta^{18}\text{O}$  value of unit TL-2 occur around 5300, 4800, 3690, and 2400 yr BP (fig 25). Unit TL-2 follow slightly increasing trend towards the middle Holocene similar trend with relatively depleted values because this

period is part of the end of the early Holocene wet period and the start of the middle Holocene dry event. The lamina width of Bero\_2, 3, 4 as shown in fig.24, follows opposite trend with the  $\delta^{18}\text{O}$  record between 5850-5890, 5440-5300, 4850-4790, and 4550 to 4390 yr BP. The lamina width decreases in periods of enriched  $\delta^{18}\text{O}$  values, interpreted as relatively dry periods, and it increases as the  $\delta^{18}\text{O}$  values get depleted interpreted as wet periods. This trend of lamina width further supports the interpretation for  $\delta^{18}\text{O}$  values of stalagmite and unit TL-2. The isotopic trends of the lake records between 4400 yr BP to present, 5845-5440, and 7353- 5880 coincides with the major hiatuses of Bero\_1 stalagmite. The  $\delta^{18}\text{O}$  value of Lake Tilo from 4400 to present show relatively depleted values at 3640-3170, 2360-3700, and 1290-700 yr BP and this periods could be interpreted as relatively wet. Similarly enriched  $\delta^{18}\text{O}$  values were recorded around 2000, and in after 700 yr BP, which could be correlated with dryer conditions.

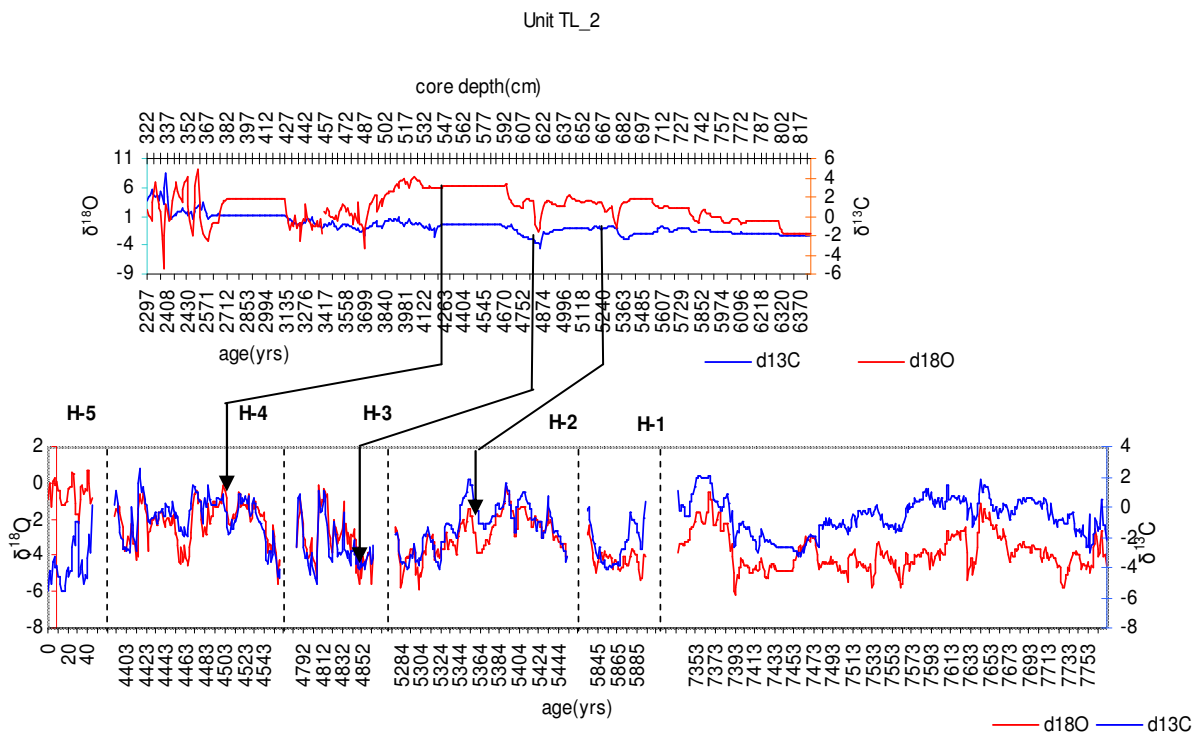


Figure 25: Bero\_1 Vs Lake Tilo Holocene isotope trends, arrows showing points of major isotope changes.

#### 4.10.5 Bero\_1 stalagmite Vs Lake Awassa isotope record

The Lake Awassa  $\delta^{18}\text{O}$  isotope record (fig 21) initially shows a sharp drop from  $\sim +5\text{‰}$  at 7130 yr BP to  $-1\text{‰}$  at around 6000 yr BP in the early-middle Holocene. It then shows a sharp rise to  $\sim +7\text{‰}$  at  $\sim 4600$  yr BP in the middle Holocene followed by a gradual decrease in  $\delta^{18}\text{O}$  values from  $+6\text{‰}$  to  $+3\text{‰}$  at around 2800 yr BP in the late Holocene. All the major isotopic trends of Lake Awassa are nearly similar with the isotopic trends of Bero\_1 stalagmite in the Holocene (fig 26). The peak isotopic value in the Lake Awassa record around 6400 yr BP coincides with the hiatus between Bero growth phase\_1 and 2. The relatively depleted isotopic value  $< -4\text{‰}$  in Bero growth phase\_2, from 5894-5834 coincides with the relatively depleted isotopic record in the Lake Awassa record around early-middle Holocene and with the hiatus between growth phase\_2 and 3. Again, the major event of isotopic enrichment in the Lake Awassa  $\sim +7\text{‰}$  record at  $\sim 4800$ , is marked by a similar major  $\delta^{18}\text{O}$  change in Bero growth phase\_4 around 4807 yr BP. The heaviest  $\delta^{18}\text{O}$  value in Bero-1 stalagmite  $\sim 0\text{‰}$  occurs at around 4505 yr BP, and similarly, the peak  $\delta^{18}\text{O}$  value  $\sim +7\text{‰}$  for Lake Awassa is recorded nearly at the same period with that of Bero. Based on the discussion in 4.2.1 section, the heaviest  $\delta^{18}\text{O}$  values for both lake Awassa and Bero\_1 stalagmite are interpreted as more dry or low humidity periods and those periods with relatively depleted  $\delta^{18}\text{O}$  are interpreted as relatively wet/more humid periods.

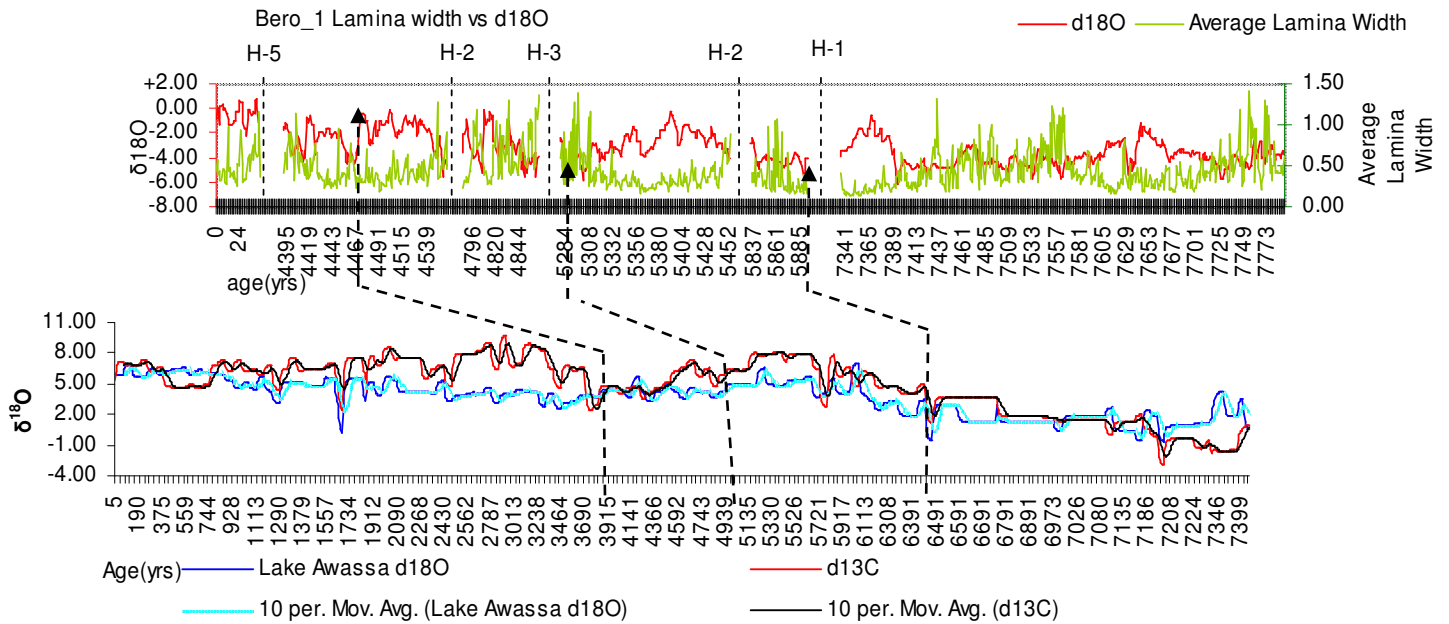


Figure 26: Lake Awassa isotope (red line) Vs Bero\_1 isotope comparison

#### 4.10.6 Comparison of Lake level variation with Speleothem isotope trends

According to the reconstructions of lake Ziway-Shalla level (Mohammed et al., 2004), the period early-mid Holocene is generally characterized by wet climate and high lake level stand and the last 5000 years is generally characterized by lower lake level stands. Yet, there were lake level evidences that showed very large but short lived dry events that interrupted the wet early Holocene.

A comparison is made between the lake level fluctuation data and stalagmite isotope record fluctuations (that of Bero\_1  $\delta^{18}\text{O}$  data) assuming that Bero\_1  $\delta^{18}\text{O}$  data is influenced by amount of precipitation, where the isotope record varies oppositely to the precipitation amount.

Relatively more depleted  $\delta^{18}\text{O}$  values were recorded in humid periods of the Holocene and enriched  $\delta^{18}\text{O}$  values were recorded in relatively low precipitation periods. The Ziway-Shalla Lake level also responded to the moisture variability in the Holocene (Lamb et al., 2000; Mohammed et al., 2004). Paleo lake level reconstructions showed Lake Ziway and Shala once merged in the middle Holocene, and over flown as a result of humid early Holocene climate (Mohammed et al., 2004). Similarly reduced lake level was recorded in arid periods of the Holocene, at 8.7-8.1, 6.7, and 5.7-5.1 Kyr, due to reduced precipitation/humidity conditions. Based on this, we can compare the  $\delta^{18}\text{O}$  variation of Bero\_1 stalagmite, in terms of precipitation amount variation and change in lake levels.

We can see clear events of shift in isotopic values in the early-middle-late Holocene coincide with the major Holocene lake level variations. Depleted  $\delta^{18}\text{O}$  values of Bero\_1 stalagmite at 7630-7330, correlate with the general early Holocene humid period reconstructed from the lake level variations.

At 5.5-4.5 cal Kyr, was the major mid Holocene dry event where the Ziway-Shalla Lake level had drastically fallen (Lamb et al., 1999; Mohammed et al., 2004). This period overlaps with the Bero\_1 growth phase 2, 3 and 4. The enriched peak isotopic records around 5392, 4809, 4550, 4880, and 4414 yr BP may be indicative of this major dry event. The mid Holocene dry event recorded by century scale lake level drop will be further resolved with the high resolution  $\delta^{18}\text{O}$  records from Bero-growth phase\_2, 3 and 4 to identify the timing, duration of relatively short lived climate events.

As discussed previously, the depleted/lighter  $\delta^{18}\text{O}$  value in Bero\_1 stalagmite corresponds with relatively higher amounts of precipitation, and this may indicate periods of increased precipitation and relatively short-lived wet events within the major mid Holocene dry event marked by the rapid lake level drop.

Around 6.7cal Kyr there was regressive event marking a minor lowering of the Ziway-Shalla lake level (Mohammed et al., 2004). This timing coincides with the major hiatus between growth phase\_1 and 2 (H-1) where the enriched  $\delta^{18}\text{O}$  values towards the end of growth phase\_1 may indicate relatively dry event. Even if the lake level drop was minor, the hiatus in Bero\_1 stalagmite is~ 1440 years long.

There were major periods of wetness at 6.3-5.1 cal Kyr, where the Ziway and Shalla lakes merged (Mohammed et al., 2004). This wet period coincides with the  $\delta^{18}\text{O}$  records of Bero growth phase\_2 and 3. The wet and high lake level stand between 6.3-5.1 cal Kyr is compared with the stalagmite isotopic record fluctuations which showed variable  $\delta^{18}\text{O}$  trends in the case of Bero growth phase\_2 and 3. This major wet event shows similarity with depleted  $\delta^{18}\text{O}$  values in Bero\_1 stalagmite around 5850-5880 and 2550-5330. Relatively enriched  $\delta^{18}\text{O}$  values  $\sim -0.5\text{‰}$  are recorded in the rest of the Bero\_1 stalagmite between 5350-5450, which indicates relatively dryer condition.

The  $\delta^{18}\text{O}$  values in phases\_4 and\_5 generally show low frequency but relatively high intensity isotopic variations. The periods of enriched  $\delta^{18}\text{O}$  values in the Bero growth phase\_4 and 5 may indicate relatively dry episodes that may have interrupted the 6.3-5.1 cal Kyr wet event recorded by high lake level stand.

The stalagmite records show the low frequency and low amplitude events at high resolution which are not detected by the lake level fluctuations. In addition, the major events of Holocene climate variation are also recorded by other proxies from Lake Tilo  $\delta^{18}\text{O}$  isotope records and also from buried soil records from Tigray, northern Ethiopia (Dramis et al., 2002; Mohammed et al., 2004).

Compared with the Ziway-Shalla lake level fluctuation, Lake Awassa isotope records also respond in similar manner showing depleted  $\delta^{18}\text{O}$  values in the early-mid Holocene, until it is gradually interrupted by rise in  $\delta^{18}\text{O}$  isotopic values around mid Holocene. The isotope record after the mid Holocene dry event shows enrichment until late Holocene. Depleted  $\delta^{18}\text{O}$  values in Lake Carbonate sediments generally indicate higher P/E condition showing relatively wet, humid and low evaporation conditions during early-mid Holocene and enriched  $\delta^{18}\text{O}$  values show lower P/E ratio showing relatively dry conditions. This is in agreement with the early-mid Holocene high lake level stand followed by late Holocene lower Ziway-Shalla lake level.

From the above discussions, it can be summarized that the speleothem  $\delta^{18}\text{O}$  values of Bero\_1 stalagmite and the lake  $\delta^{18}\text{O}$  records follow variations in the same direction. But the magnitudes and the frequency of variation are not similar.

The stalagmite  $\delta^{18}\text{O}$  records are characterized by five major trends of variation at 100-120 years each interrupted by hiatuses and there are smaller variations at 10-20 years time scale within the

major isotopic trends. The  $\delta^{18}\text{O}$  value from the lake Tilo and Awassa records also follow similarly increasing trend towards the middle Holocene. These Holocene  $\delta^{18}\text{O}$  variations of the speleothem and lake records show nature of precipitation/humidity variability as previously reconstructed lake level variations showed the Holocene precipitation variations.

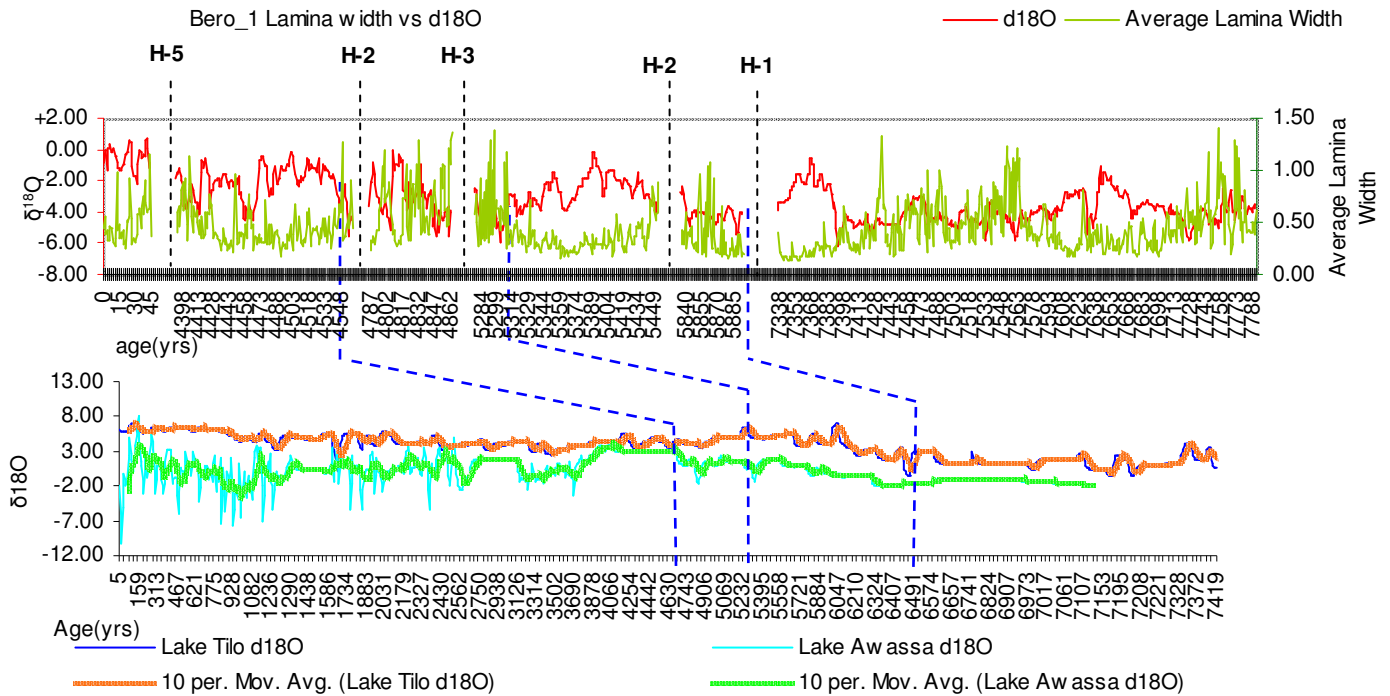


Figure 27: Lake Awassa, Lake Tilo and Bero\_1 stalagmite Holocene isotope trends.

## Chapter 5: Conclusion and Recommendation

### 5.1 Conclusions

- ✓ All  $\delta^{18}\text{O}$  values of the stalagmites are poorly correlated to each other and the lake isotope records are similarly poorly correlated through out the Holocene.
- ✓ Comparison of modern and Holocene age stalagmites showed stalagmites from the same region may respond differently, and even if they show similar trend of variation, the response of the isotopic value is with different amplitude.
- ✓ The poor correlation between the lake and stalagmite isotope records is because they respond to different climate forcing, the lake  $\delta^{18}\text{O}$  mainly responds to evaporative enrichment, and the  $\delta^{18}\text{O}$  records of stalagmite calcite mainly responds to precipitation amount.
- ✓ Comparison of lake and stalagmite isotope records shows both records are poorly correlated to each other. But still the Holocene isotopic trends together with lamina width and lake level variations change in the same direction at different sensitivities.
- ✓ All the speleothem isotope and lamina width records and the Ziway-Shalla Paleo-lake level fluctuation data show similar trend of variation through out the Holocene. Never the less, still the high resolution  $\delta^{18}\text{O}$  data obtained from the speleothem records show additional small scale climate perturbations which could be only locally significant.
  
- ✓ The difference between the isotopic trends in stalagmite records is due to local effects related to drip water flow and residence time, and similarly the some non climatic effects related with groundwater inflow in to lake Tilo was observe during the early Holocene.
- ✓ The stable isotope and lamina width data from the stalagmite is used to refine the generally wet early Holocene condition evidenced from the lake level data. In this regard, the initial growth phase of Bero\_1 stalagmite, which coincides with the early Holocene wet condition, there were peak values of  $\delta^{18}\text{O}$  at 7365-7395 and 7641-7675 yr BP which may coincide with sort lived dry episodes, and highly depleted values were recorded at 7393-7396, 7561-7565, and 7729-7733, which may indicate the maximum wet events in the early Holocene. In addition, the mid Holocene wet interval between 6.3-5.1 cal Kyr was also interrupted by brief dry events at 5345-5358 and 5388-5397 yr BP.

- ✓ According to the comparison made between the trends of speleothem and lake records, there were five major isotopic trends observed in the speleothem variations at a time scale of 100-120 years with small scale variations at 10-20 years time scale within the major trends.

## **5.2 Recommendations**

The annually laminated high resolution stalagmite records from the Mechara karst area are one of the best palaeoclimate archives with precise radiometric dating advantages and suitable internal stratigraphy. Hence it is recommended to work more on the stalagmite in order to fill the gaps/hiatuses in Bero\_1 stalagmite and to have the full Holocene  $\delta^{18}\text{O}$  variability. It is also important to include other proxies like pollen in the stalagmites so that a comparison will be made with other lake records to see the vegetation change in the Holocene, and hence determining the effect of vegetation change on local climate. It will be important to have a high resolution climate record in this period so that important climate models will be prepared to understand the precipitation and drought variation in the Holocene in Ethiopia and make future predictions. Hence, it is recommended to work more on the multi-proxy climate data that stalagmites provide.

## References

- Araguas A.L., Froehlich K., Rozanski K. 2000., deuterium and oxygen-18 isotope composition of precipitation and atmospheric moisture. *Hydrological Process* 14: 1341-1355.
- Asrat A., Baker A., Umer M., Leng M. J., van Calsteren P., and Smith C., 2007. A high-resolution multi-proxy stalagmite record from Mechara, Southeastern Ethiopia: palaeohydrological implications for speleothem palaeoclimate reconstruction. *J. Quatern. Sci.* 22(1), 53–63.
- Asrat A., Baker A., Leng M.J., Gunn J. and Umer M., 2008. Environmental Monitoring in the Mechara caves Southeastern Ethiopia: Implications for Speleothem Palaeoclimate Studies. *International Journal of Speleology*, 37(3), 207-220.
- Ayalon A., Bar-Matthews M., Kaufman A., 1999. Petrography, strontium, barium and uranium concentrations, and strontium and uranium isotope ratios in speleothems as palaeoclimate proxies: Soreq Cave, Israel. *The Holocene* 9: 715-722
- Baker A., 1998. Testing theoretically predicted stalagmite growth rate with recent annually laminated samples: Implications for past stalagmite deposition. *Geochimica et Cosmochimica Acta* 62, 3: 393-404.
- Baker A., Genty D., 1999. Fluorescence wavelength and intensity variation of cave waters. *Journal of Hydrogeology* 271: 19-34.
- Baker A., 2002. Spectrophotometric discrimination of river dissolved organic matter. *Hydrological Processes* 16: 3203-3213.
- Baker A., Asrat A., Fairchild I.J., Wynn P.M., Bryant C., Genty D., and Umer M., 2007. Analysis of the climate signal contained in  $\delta^{18}\text{O}$  and growth rate parameters in two Ethiopian Stalagmites. *Geochimica et Cosmochimica Acta*, 71: 2975-2988.
- Baker A., Asrat A., Fairchild I.J., Leng M.J., Wynn P.M., Bryant Charlotte., Genty D., Umer M., 2008. Analysis of the climate signal contained within  $\delta^{18}\text{O}$  and growth rate parameters in two Ethiopian stalagmites. *Geochimica et Cosmochimica Acta* 71: 2975-2988.

- Bar-Matthews M., and Ayalon A., 1997. Late Quaternary palaeoclimate in the Eastern Mediterranean Region from Stable Isotope Analysis of Speleothem at Soreq Cave, Israel. *Quaternary Research* 47: 155-168.
- Bar-Matthews M., Ayalon A., Gilmour M., Matthews A., Hawkesworth C.J., 2003. Sea-land oxygen isotopic relationships from planktonic foraminifera and speleothems in the eastern Mediterranean region and their implications for paleorainfall during interglacial intervals. *Geochimica et Cosmochimica Acta*. 67,17, 3181-2003.
- Bertaux J., Sondag F., Santos R., Soubies F., Causse C., Plagnes V., Cornec P.L., Seidel A., 2002., Paleoclimatic record of speleothems in a tropical region: study of laminated sequences from a Holocene stalagmite in Central-West Brazil. *Quaternary International* 89: 3-16.
- Blyth A. J., Farrimond P., Jones M., 2006. An optimized method for the extraction and analysis of lipid biomarkers from stalagmites. *Organic Geochemistry* 37: 882-890.
- Bonnefille, R., Mohammed, U., 1994. Pollen inferred climatic fluctuations in Ethiopia during the last 3,000 years. *Palaeogeography, Palaeoclimatology, Palaeoecology* 109, 331–343.
- Burns S.J., Fleitmann D., Matre A., Jan K., Al-Subbary Abdulhakim A., 2003. Indian Ocean Climate and an Absolute Chronology over Dansgaard/Oeschger Event 9 to 13. *Science* 301: 1365-1367.
- Cia Y., An Z., Cheng H., Edwards R.L., Kelly M.J., Liu W., 2006. High-resolution absolute-dated Indian Monsoon record between 53 and 36 Ka from Xiaobailong Cave, Southwestern China. *Geological Society of America* 34, 8: 621-624.
- Darling W.G, and Talbot C.J., 2003. The O and H stable isotope composition of fresh waters in the British Isles. 1. Rainfall. *Hydrology and Earth System Science*, 163-181.
- Darbyshire, I., Lamb, H.F. and Umer, M., 2003: Forest clearance and regrowth in northern Ethiopia during the last 3000 years. *The Holocene* 13, 553–62.
- Desmarchelier J.M., Hellstrom J.C., McCulloch M.T., 2006. Rapid trace element analysis of speleothems by ELA-IPC-MS. *Chemical Geology* 231: 102-117.

- Doralle J.A., Edwards R.L., Onac B.P., 2001. Stable Isotope as Environmental Indicators in Speleothems. Final report of IGCP: 379, 2001, 107-120.
- Dramis F., Umer M., Calderoni G., Haile M., 2003. Holocene climate phases in Tigray (northern Ethiopia): comparison with lake level fluctuations in the Main Ethiopian Rift. *Quaternary Research*, 60: 274-283.
- Emiliani Cesare., 1966. Isotope Paleotemperatures. *Science* 18: 145, 851-857.
- Fairchild I.J., Borsato A., Tooth A.F., Frisia S., Hawkesworth C.J., Huang Y., McDermott F., Spiro B., 2000. Controls on trace element (Sr-Mg) compositions of carbonate cave waters: implications for speleothem climate records. *Chemical geology* 166: 255-269.
- Fairchild I.J., Baker A., Borsato A., Frisia S., Hinton R.W., McDermott F., Tooth A.F., 2001. *Journal of the Geological Society, London* 158: 831-841.
- Fairchild A.A., Shaw P.A., Holmgren K., Thorp-Lee j., 2003. Corroborated rainfall records from aragonitic stalagmites. *Earth and Planetary Science Letters* 215: 265-273.
- Fairchild I. J, Smith CL, Baker A, Fuller L, Spotl C, Matthey D, McDermott F, E. I. M. F. 2006a., Modification and preservation of environmental signals in speleothems. *Earth Science Reviews*: 75: 105–153.
- Fairchild I. J., Tuckwell G. W., Baker A., and Tooth A. F., 2006b Modelling of dripwater hydrology and hydrogeochemistry in a weakly karstified aquifer (Bath, UK): implications for climate change studies. *J. Hydrol.* 321, 213–231.
- Fleitmann D., Burns S.J., Neff U., Mudelsse M, Mangini A., Matter A., 2003. Palaeoclimatic interpretation of high-resolution oxygen isotope profiles derived from annually laminated speleothems from Southern Oman. *Quaternary Science Review* 23: 935-945.
- Freidman I. and O'neil J., 1977. *Data of Geochemistry*, 1977. United States Government Printing Office, KK1-KK12.
- Frisia S., Borsato A., Preto N., McDermott F., 2003. Late Holocene annual growth in three Alpine stalagmites records the influence of solar activity and the North Atlantic Oscillation on winter climate. *Earth and Planetary Science Letters* 216: 411-424.

Genty D., and Massuault M., 1999., Carbon transfer dynamics from bomb-  $^{14}\text{C}$  and  $\delta^{13}\text{C}$  time series of a laminated stalagmite from SW France-Modelling and comparison with other stalagmite records. *Geochimica et Cosmochimica Acta* 63: 1537-1548.

Genty D., Plagnes V., Causse C., Cattani S.M., Falourd S., Blamart D., Ouahdi R., Van-Exter S., 2001., Fossil water in large stalagmite voids as a tool for isotope composition reconstruction and paleotemperature calculation. *Chemical Geology* 184: 83-95.

Genty D., Blamart D., Ghaleb B., Plagnes V., Causse Ch., Bakalowicz M., Zouari K., Chkir N., Hellstorm J., Wainer K., Bourges F., 2006., Timing and dynamics of the last deglaciation from European and North African  $\delta^{13}\text{C}$  stalagmite profiles-comparison with Chinese South hemisphere Stalagmites. *Quaternary Science Reviews* 25: 2118-2142.

Hellstorm J., McCulloch M., Stone J., 1998. A Detailed 31,000-Year Record of Climate and Vegetation Change, from the Isotope Geochemistry of Two New Zealand Speleothems. *Quaternary Research* 50: 167-178.

Huang Y and Fairchild I.J., 2000. Portioning of  $\text{Sr}^{2+}$  and  $\text{Mg}^{2+}$  into calcite under karst-analogue experimental conditions. *Geochimica et Cosmochimica Acta* 65: 47-62.

Johnson K.R., Hu C., Belshaw N.S., Henderson G.M., 2006. Seasonal trace-element and stable isotope variations in a Chinese speleothem: The potential for high resolution paleomonsoon reconstruction. *Earth and Planetary Science Letter* 244: 394-407.

Kaufmann G and Dreybrodt W., 2004. Stalagmite growth and palaeo-climate: an inverse approach. *Earth and planetary Science Letters*: 224, 2004, 529-545.

Lamb A. L., Leng, M.J., Lamb, H.F., Umer, M.U., 2000. A 9000-year oxygen and carbon isotope record of hydrological change in a small Ethiopian crater lake. *The Holocene* 10, 167-177.

Lamb H.F., 2001. Multi-proxy Records of Holocene Climate And Vegetation Changes From Ethiopian Crater Lakes. *Biology And Environment, Proceedings of the Royal Irish Academy*, Vol. 101B. No.1-2., 35-46.

- Lamb A. L., Leng M.J., Lamb H.F., Telford R.J., Mohammed M.U., 2002. Climatic and non-climatic effects on  $\delta^{18}\text{O}$  and  $\delta^{13}\text{C}$  compositions of Lake Awassa, Ethiopia, during the last 6.5 Ka. *Quaternary Science Review* 21: 2199-2211.
- Lamb H.F., Leng M.J., Telford R.j., Ayanew T., Umer M., 2006. Oxygen and carbon isotope composition of authigenic carbonate from an Ethiopian lake: a climate record of the last 2000 years. *The Holocene*: 17, 2007. 515-124.
- Lauritzen S. and Lundberg J.,1999. Speleothems and climate: a special issue of the Holocene. *The Holocene*: 9, 1999. 643-647.
- Lieng H., Lauritzen S.E., Lundberg J., 2001. Stable Isotope Stratigraphy of a Late Last Interglacial Speleothem from Rana, north Norway. *Uaternary Research* 56: 155-164.
- Matthews M.B., Ayalon A., Sass E., Halicz L., 1996. Carbonand Oxygen isotope study of the active water-carbonate system in a Karstic Mediterranean cave: Implications for palaeoclimate research in semiarid regions. *Geochimica et cosmochimica Acta* 60: 337-347.
- McGarry S.F., Baker A., 2000. Organic acid fluorescence: application to speleothem palaeoenvironmental reconstruction. *Quaternary Science Reviews* 19: 1087-1101.
- McDermott F., 2004. Paleo-climate reconstruction from stable isotope variations in speleothems: a review. *Quaternary Science Reviews* 23: 901-918.
- Mickler PJ, Banner JL, Stern L, Asmerom Y, Edwards RL, Ito E. 2004. Stable isotope variations in modern tropical speleothems: evaluating equilibrium vs. kinetic isotope heffects. *Geochimica Cosmochimica Acta* 68: 4381–4393.
- Mickler P.J., Stern L.A., Banner J.L., 2006. Large kinetic isotope effects in modern speleothems. *Geological Society of America* 118: 65-81.
- Mohammed, M.U., Bonnefille, R., 1998. A Late Glacial to Late Holocene pollen record from a highland peat at Tamsaa, Bale Mountains, South Ethiopia. *Global and Planetary Change* 16-17, 121–129.

- Mohammed MU, Legesse D, Gasse F, Bonnefille R, Lamb HF, Leng M, Lamb AL. 2004. Late Quaternary climate changes in the Horn of Africa. In *Past Climate Variability through Europe and Africa*, Battarbe RW (ed.). Springer-Verlag: Dordrecht; 159–180.
- Proctor C.J., Baker A., Barnes WL., 2002. A three thousand year record of North Atlantic climate. *Climate Dynamics* 19: 449-454.
- Solomon Kassa., 2007. Rainfall Variation During The Last Century As Characterized By Stable Isotopes And Trace Elements In A Modern Speleothem From Mechara Karst-Southeastern Ethiopia. Unpublished Ms.C Thesis, Addis Ababa University, Ethiopia.
- Thompson P., Schwartz H.P., Ford D.C., 1974. Continental Pleistocene climate variations from Speleothem Age and Isotope Data. *Science, New Series*, 184: 893-895.
- Tooth A.F and Fairchild I.J., 2003. Soil and karst hydrology controls on the geochemical evolution of speleothem-forming drip waters, Crag Cave, southwest Ireland. *Journal of Hydrology* 273: 51-68.
- Umer, M., Lamb, H., Bonnefille, R., Le´zine, A.-M., Tiercelin, J.-J., Gibert, E., Cazet, J.P., Watrin, J., 2007. Late Pleistocene and Holocene vegetation history of the Bale Mountains, Ethiopia, *Quaternary Science Reviews*.
- Verheyden S., Keppens E., Fairchild I.J., McDermott F., Weis D., 2000. Mg, Sr and Sr isotope geochemistry of a Belgian Holocene speleothem: implications for palaeoclimate reconstructions. *Chemical Geology* 169: 131-144.
- Williams P.W., Marshall A., Ford D.C., Jenkinson A.V., 1999. Palaeoclimate interpretation of stable isotope data from Holocene speleothems of the Waitomo district, North Island, New Zealand. *The Holocene* 9, 6: 649-657.
- Williams P.W., King D.N.T., Zhao J-X., Collerson K.D., 2004. Speleothem master chronologies: combined Holocene 18O and 13C records from the Northern Island of New Zealand and their palaeoenvironmental interpretations. *The Holocene* 14,2: 194-208.
- Xia Q., Zhao X.J., Collerson K.D., 2001. Early-Mid Holocene climatic variations in Tasmania, Australia: multi-proxy records in a stalagmite from Lynds Cave. *Earth and Planetary Science Letter* 194: 177-187.

## **DECLARATION**

I the undersigned declare that this thesis is my original work, has not been presented for a degree in any other university and that all sources of material used for the thesis have been duly acknowledged.

Aynalem Zenebe Degefa

School of Graduate Studies

The thesis has been submitted for examination with my approval as university advisor.

Asfawossen Asrat (PhD) \_\_\_\_\_